수의학박사 학위논문

Role of Mettl14 in Liver Regeneration after Partial Hepatectomy in Mouse Model

Mettl14 유전자 형질전환 마우스를 이용한 간 재생의 억제 기전 연구

2023 년 8 월

서울대학교 대학원

수의학과 수의생명과학 전공

(수의발생유전학)

양 인 숙

A Dissertation for the Degree of Doctor of Philosophy

Role of Mettl14 in Liver Regeneration after Partial Hepatectomy in Mouse Model

August 2023

Insook Yang

Supervisor: Prof. Je Kyung Seong, D.V.M., Ph.D.

Department of Veterinary Medicine

Veterinary Life Science

(Major in Veterinary Developmental and Genomics)

Graduate School of Seoul National University

Role of Mettl14 in Liver Regeneration after Partial Hepatectomy in Mouse Model

지도 교수 성 제 경

이 논문을 수의학박사 학위논문으로 제출함

2023 년 5 월

서울대학교 대학원

수의학과 수의생명과학전공

(수의발생유전학)

양 인 숙

양인숙의 수의학박사 학위논문을 인준함

2023 년 7 월

위 원 장 윤 여 성 (인)

부위원장 성 제 경 (인)

위 원 류 덕 영 (인)

위 원 이 미 옥 (인)

위 원 구 승 회 (인)

Abstract

Liver regeneration is a well-known systemic homeostatic phenomenon. The N6-methyladenosine (m^6A) modification pathway has been associated with liver regeneration and hepatocellular carcinoma. m^6A methyltransferases, such as methyltransferase 3 (METTL3) and methyltransferase 14 (ME-TTL14), are involved in the hepatocyte-specific-regenerative pathway.

To illustrate the role of METTL14 in non-parenchymal liver cells, which related in the initiation phase of liver regeneration, I performed 70% partial hepatectomy (PH) in Mettl14 hetero-zygous (HET) and wild-type (WT) mice. Next, I analyzed the ratio of liver weight to body weight and the expression of mitogenic stimulators derived from non-parenchymal liver cells. Furthermore, I evaluated the expression of cell cycle-related genes and the hepatocyte proliferation rate by immunostaining using Proliferating Cell Nucleus Antigen (PCNA) and Marker of proliferation KI-67 (MKI67) antibodies. During regeneration after PH, the weight ratio was lower in Mettl14 HET mice

compared to WT mice. The expression of hepatocyte growth factor (HGF) and tumor necrosis factor (TNF)-α, mitogens derived from non-parenchymal liver cells that stimulate the cell cycle, as well as the expression of cyclin B1 and D1, which regulate the cell cycle, and the number of MKI67 positive cells, which indicate proliferative hepatocyte in the late G1-M phase, were significantly reduced in Mettl14 HET mice 72h after PH. Our findings demonstrate that global Mettl14 mutation may interrupt the homeostasis of liver regeneration after an acute injury like PH by restraining certain mitogens, such as HGF and TNF-α, derived from sinusoidal endothelial cells, hepatic stellate cells, and Kupffer cells.

These results provide new insights into the role of Mettl14 in the clinical treatment strategies of liver disease.

.....

Keywords: Mettl14-knockkout heterozygous mice, Liver regeneration, 70% partial hepatectomy, Hepatocyte growth factor, TNF-α and non-parenchymal liver cells

Student number: 2017-29705

Table of Contents

List of Figures

List of Tables

Chapter 1.

Analysis of m^6A RNA Modification Regulators during Liver Regeneration after Partial Hepatectomy in Mice

1.1 Introduction

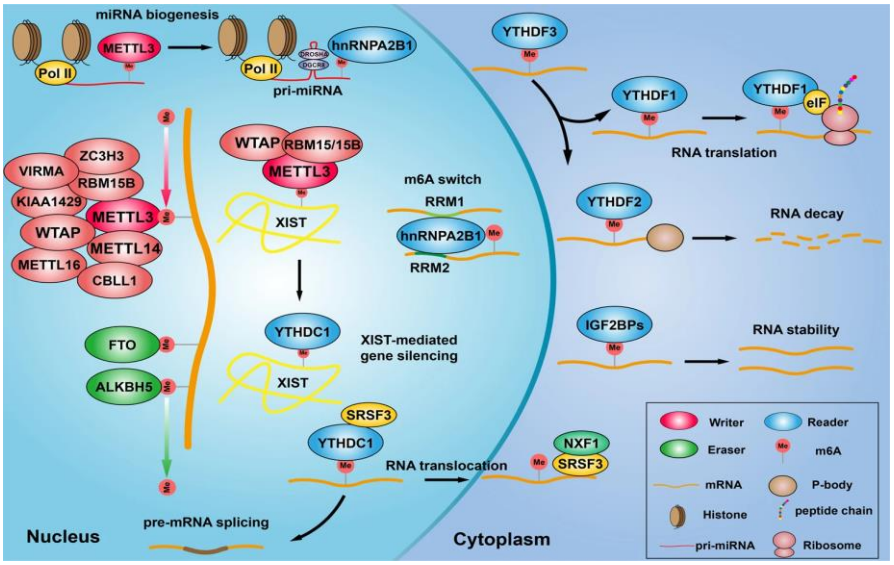

Figure 1−1. Regulation of m6A modification and its functions in RNA metabolism by m6A "writer", "eraser" and "reader" proteins (Chen Y et al., Signal Transduction and Targeted Therapy, 2021).

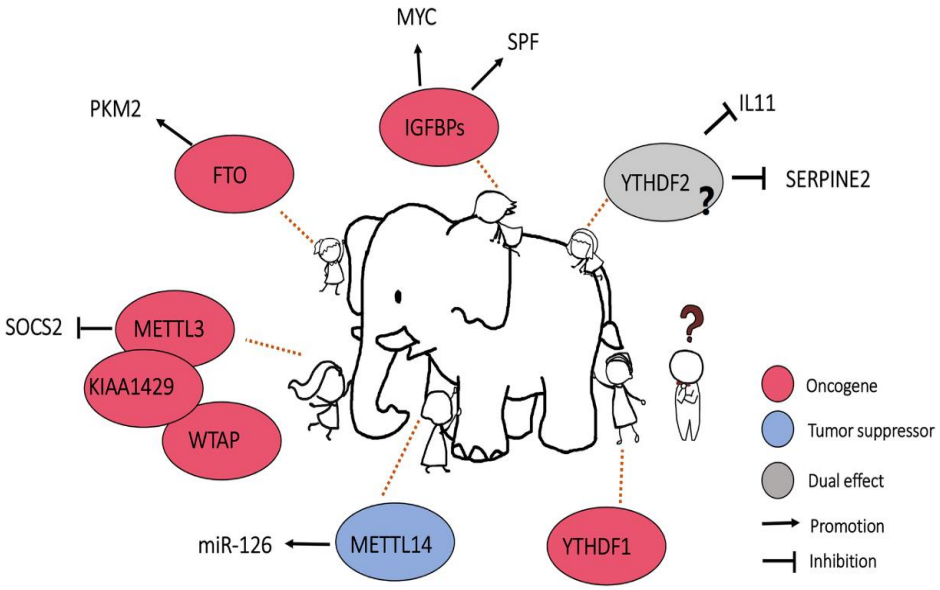

Figure 1-2. Deregulation of m6A modification and m6A regulators in human HCC (Chen M et al., Molecular cancer, 2020).

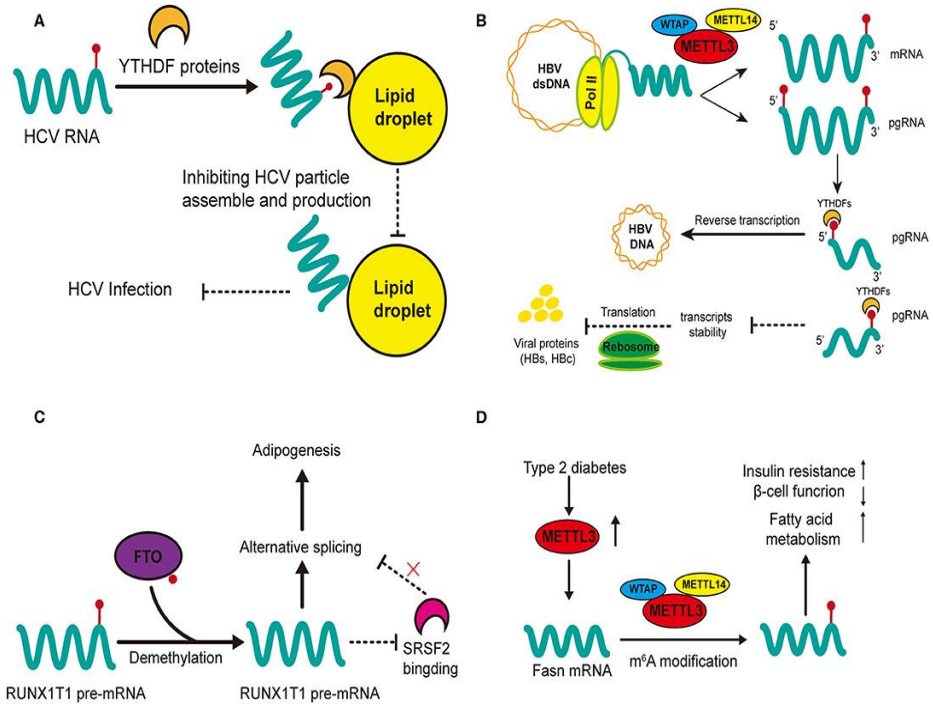

Figure 1-3. Regulatory functions of m6A in HCC-related hepatic diseases. m6A regulation in HCV (A) and HBV (B) affect viral activities (infection and replication) while m6A modification in non-alcohol fatty liver disease (NAFLD) promotes adipogenesis (C) and insulin resistance (D) (Jiahua Lu, Front. Oncol., 2020).

N6-methyladenosine (m^6A) plays a crucial role in regulating RNA stability, splicing and translation and has been shown to involve in various biological processes (Fig 1-1)[1,2]. m^6A is modified by m^6A methyltransferases (writers), such as METTL3 and METTL14, and removed by demethylases (erasers), including FTO and ALKBH5. m^6A is recognized by YTHDF and YTHDC, which are m^6A-binding proteins, also known as "readers"(Fig 1-1)[2].

As a new frontier of epigenetic research, mRNA m^6A modification has earned interesting concern, and its involvement in different biological processes and disease models has been recently reported. Since epigenetic alterations are frequently observed in human cancers, adequate evidence in the recent few years uncovering the important regulatory functions mediated by m^6A modification deserved[1].

The RNA epigenetic studies in human HCC have encountered a major problem in that some studies above have reported contradictory results on the expression patterns or functions of different m^6A regulators[3-7]. The inconsistent findings in human HCCs studies only reveals a part of the whole picture, akin to the

parable of "the blind men and the elephant" (Fig. 1-2)[1]. Further investigations have been suggested to adjust these seemingly contradictory findings to generate an integrated model[1].

Recently, it has been revealed to be associated with pathological phenomena such as stem cell differentiation, immunoregulation, and carcinogenesis, and physiological phenomena such as spermatogenesis and adipogenesis[8-12]. Moreover, it is reported that the m^6A modification pathway has been associated with hepatocellular carcinoma and liver regeneration (Fig 1-3)[2,13-16]. But, the mechanisms of the entire process related in m^6A modification pathway in liver regeneration remain unclear.

Therefore, an investigation of m^6A modification pathway in liver regeneration after PH in mice is required to deeply understand the biological phenomenon of liver regeneration.

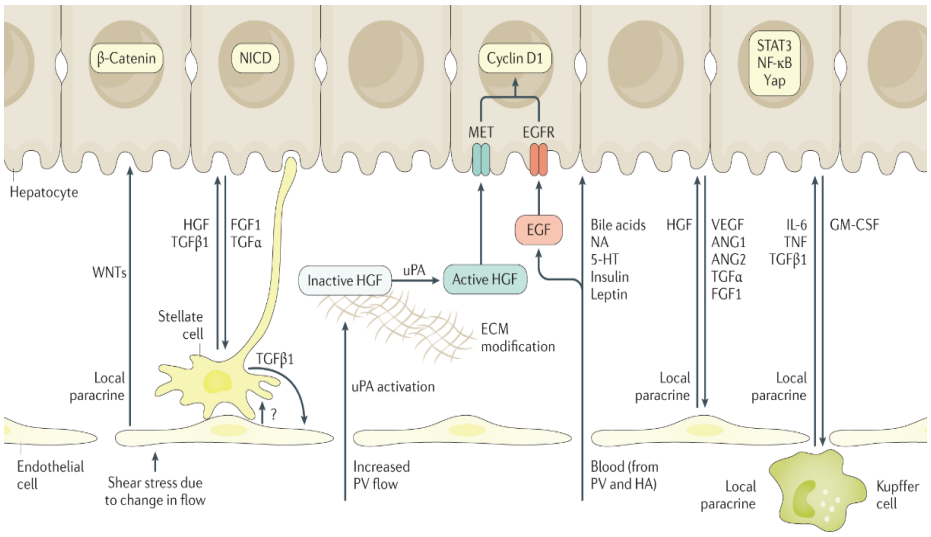

Figure 1-4. Multiple signaling molecules regulate cell proliferation during liver regeneration (George K Michalopoulos, *Nat Rev Gastroenterol Hepatol*, 2021).

The liver is a solid organ with the regenerative ability to maintain a liver weight to body weight ratio of 100% to meet metabolic demands and regulate homeostasis in the body[17,18]. Therefore, this regenerative ability of the liver renders it a useful model for biochemical, genetical, and bioengineering tools to identify molecular mechanisms and improve the medical care of liver diseases[18-26]. Molecular mechanisms of liver regeneration contain extracellular and intracellular factors to stimulate the gene transcription processes that are normally silenced in quiescent live cells[27]. Many upstream signaling pathways as well as the detailed transcriptional regulators of liver regeneration have been extensively studied (Fig.1-4)[17].

To study this pathway, I performed 70% partial hepatectomy (PH) in mice (Fig. 1-5)[28-29]. This method is the most obvious and well-known experimental technique to enable timing of the regenerative events and to induce compensatory regeneration[17,30]. It also helps to observe time-dependent changes in histological and biochemical events in a relatively short period[27,31]. After a 70% PH in rodents, the liver mass is regained within 7-8 days, with complete recovery achieved

within 3 weeks. The remnant lobes increase in size, then they reach the mass of the liver before surgery[17]. This is not the formation of new liver lobes or lobules. Postoperative liver regeneration, the lobules and biliary ductules are larger than before 70% PH and the width of the hepatocyte plates increases from one hepatocyte to 1.5 hepatocytes average, enclosed on either side by hepatic sinusoids [20-22,32].

During postoperative liver regeneration, mitogenic stimul - ators including growth factors, such as hepatocyte growth factor (HGF) and epidermal growth factor (EGF), cytokines, such as TNF-α, IL6, and hormones, such as insulin and norepinephrine, all participate in the proliferative processes (Fig. 1-6)[24-26,31,33-37]. Furthermore, in the liver regeneration process induced by acute injury, the function of cytokines such as TNF-α and IL-6 that promote regeneration and growth factors such as HGF, EGF, TGF, insulin, and glucagon are relatively clear[30,38-40].

In this study, I evaluated the expression of m^6A modification pathway related molecules, such as METTL3, METTL14, YTHDF2 and FTO, and including well-known molecules for liver regeneration after PH in mice. It may suggest that m^6A

modification pathway involved in liver regeneration after PH.

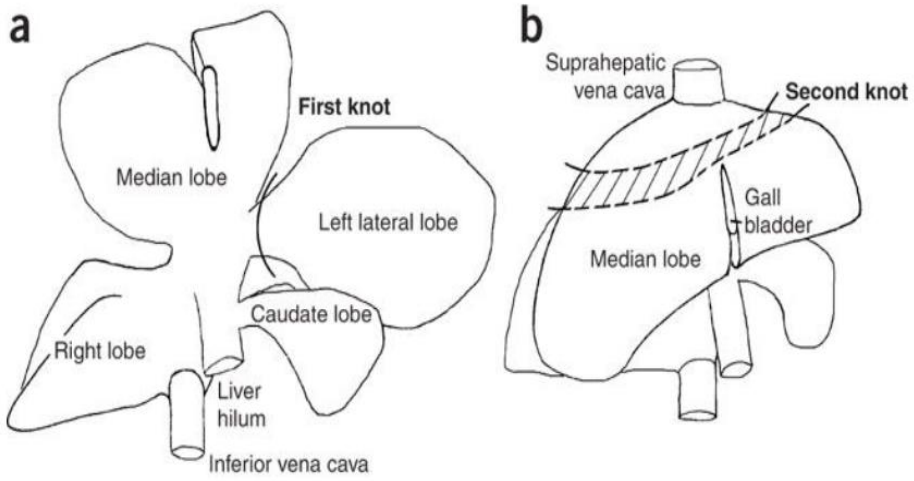

Figure 1-5. Mouse liver anatomy and positioning of silk threads for knots for 70% PH (Mitchell Claudia et al. Nat Proto, 2008).

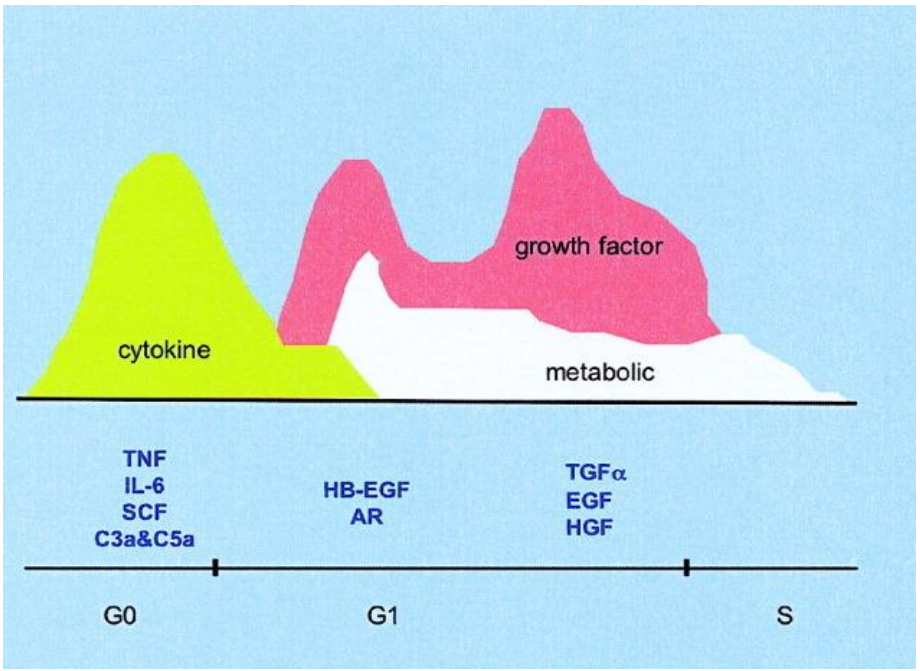

Figure 1-6. Cytokine, growth factor, and metabolic networks during liver regeneration (Nelson Fausto, Hepatology, 2006).

1.2 Materials and Methods

Animals

C57BL/6 mice purchased from the Korea Research Institute of Bioscience and Biotechnology (KRIBB) were used for all experiments in this study. Mice were maintained under a 12-h light-dark cycle and were provided with free access to water and a regular chow diet in a specific pathogen-free (SPF) facility.

Partial hepatectomy

Male mice, aged 8 to 10 weeks, were subjected to 70% partial hepatectomy under isoflurane (Hana Pharm Co., Ltd.) inhalation anesthesia according to a published protocol[28,29,41].

The left lateral and median lobe of the liver along with the gall bladder were ligated and removed. The gall bladder was always removed during surgery to avoid damage. For postoperative care, all animals were administrated 5mg/kg ketoprofen (Daehan Inc., Korea) intraperitoneally to control pain. All mice were sacrificed at the indicated time. The weight of the remnant livers was measured, which were then subsequently fixed in 4%

paraformaldehyde and snap-frozen in liquid nitrogen immediately after extraction. Animal experiments were performed following the "Guide for Animal Experiments" edited by the Korean Academy of Medical Sciences and "ARRIVE Guidelines" by NC3Rs and approved by the Institutional Animal Care and Use Committee of Seoul National University, Seoul, Korea (IACUC approval no. SNU-190919-9).

m^6A quantification

The m^6A level in total RNA in the liver tissues was assessed using the EpiQuikTM m^6A RNA Methylation Quantification Kit (cat. P-9005; Epigentek Group Inc., USA) following the manufacturer's protocol. Total RNA (200 ng) was added to each well, followed by the addition of the capture antibody solution and detection antibody solution[3]. The absorbance at 450 nm was colorimetrica- lly measured to determine the m^6A level.

Histology and Immunohistochemistry

Liver tissues were fixed overnight in 4% paraformaldehyde, embedded in paraffin, and used for hematoxylin and eosin (H&E)

staining, as well as immunostaining with antibodies against PCNA (cat. ab92552; Abcam, Cambridge, UK). The immunostaining was developed with diamino-benzidine. To quantify hepatocyte proliferation after immunostaining, 10 fields per slide were randomly chosen under the microscope to count the PCNA-positive hepatocytes and calculate the percentage of PCNA-positive hepatocytes among the total hepatocytes in each field. Mitotic hepatocytes were counted in 10 fields per slide of H&E-stained hepatocytes. Following the mitotic figures defined by Baak, mitotic cells were counted based on nuclear morphology under a microscope. The mitotic index was defined as the mean number of mitotic cells in 10 fields[42].

Western blotting

Protein lysates were prepared in RIPA buffer containing 0.5 mM phenylmethane sulfonyl fluooride (PMSF), 4 μg/ml leupeptin, 4 μg/ml aprotinin, and 4 μg/ml pepstatin, separated by sodium dodecyl sulfate (SDS)-polyacrylamide gel electrophoresis (PAGE), and transferred to polyvinylidene fluoride (PVDF) membranes. Membranes were incubated with the following

primary antibodies overnight: METTL3 (cat. 96391, Cell Signaling Technology, MA, USA), METTL14 (cat. HAP038002; Sigma-Aldrich, MO, USA), YTHDF2 (cat. ab220163), TNF-α (cat. 11948, Cell Signaling Technology), HGF (cat. ab83760), EGFR (cat. 2646; Cell Signaling Technology), Cyclin B1 (cat. 12231; Cell Signaling Technology), Cyclin D1(cat. 2978; Cell Signaling Technology), CDK4 (cat. Sc-23896; Santa Cruz Biotechnology, Inc., USA), GAPDH (cat. 2118, Cell Signaling Technology) then incubated with the secondary antibody goat-anti-rabbit-HRP or goat-anti-mouse-HRP for 1h. Antibody binding was visualized using the Pierce TM ECL western blotting detection system (Chemi-Doc XRS+System; Bio-rad, CA, USA).

mRNA isolation and real-time polymerase chain reaction (RT-PCR)

Total RNA was isolated from the liver using Trizol (Ambion, TX, USA) reagent. RT-PCR analysis of the isolated mRNA was performed in a two-step reaction [43]. In the first step, a complementary DNA strand was synthesized using the

AccuPower® RT reverse transcription kit (Bioneer, Daejeon, South Korea), and the second step was performed on a 7500 Real-Time PCR System (Applied Biosystems, MA, USA) with SYBR green (BIO-94020; Bioline, Toronto, Canada) and specific primers for each of the target genes. Each assay included the *36B4* gene as an endogenous reference. Gene expression was calculated using the

$2^{-\triangle\triangle CT}$ method.

Statistical analysis

Statistical analysis was performed using GraphPad Prism 7.0 (GraphPad Software, La Jolla, CA, USA). Data are presented as mean ± standard deviation (SD). Statistical significance among more than two groups was assessed using Student's t-test. A P-value less than 0.05 was considered statistically significant.

Table 1. Primers used for Real-Time PCR analysis

Target gene	Forward (5' →3')	Reverse (3'→5')
HGF	CTGCTTCATGTCGCCATCC	TGGGTCTTCCTTGGTAAGAGTAG
EGF	TTCTCACAAGGAAAGAGCATCTC	GTCCTGTCCCGTTAAGGAAAAC
IL-6	CTTCCATCCAGTTGCCTTCTTG	AATTAAGCCTCCGACTTGTGAAG
TNF-α	CCCACTCTGACCCCTTTACT	TTTGAGTCCTTGATGGTGGT
Cyclin A1	AGCAGGCTGTGGCTTACTAG	CCTAGCACGGTTCTCTGTGG
Cyclin B1	CAGCGAAGAGCTACAGGCAAG	CTCAGGCTCAGCAAGTTCCA
Cyclin D1	CGCAAAGAGGAAGGAGCCAGC	CCTACTCTCAGGGTGATGCAGATTC
Mettl3	CTGGGCACTTGGATTTAAGGAA	TGAGAGGTGGTGTAGCAACTT
Mettl14	CTGAGAGTGCGGATAGCATTG	GAGCAGATGTATCATAGGAAGCC
YTHDF2	GAGCAGAGACCAAAAGGTCAAG	CTGTGGGCTCAAGTAAGGTTC
FTO	TTCATGCTGGATGACCTCAATG	GCCAACTGACAGCGTTCTAAG

1.3 Results

1.3.1. 70% PH facilitates liver regeneration in C57BL/6 mice

To study the liver regeneration, I performed 70% PH according to a published protocol in C57BL/6 mice (Fig.1-7 A-C)[28,29]. I performed aseptic surgery under inhalation anesthesia and analgesic administration. I first determined the enlargement of remnant liver lobes after PH (Fig.1-7 D). I assessed liver regeneration by measuring the ratio of liver weight to body weight for 7 days after surgery. I found a significantly increased ratio which reached 86% of the pre-surgical liver mass within 7 days after PH (Fig. 1-8). The level of alanine aminotransferase (ALT) and aspartate aminotransferase (AST), biomarkers of liver function, were increased during 6h between 48 h after PH and recovered close to the pre-surgical level at 72 h after PH in mice (Fig. 1-9).

I then conducted an additional experiment to analyze the effect of PH on cell proliferation using immunostaining of PCNA as a marker of proliferating cell nuclei (Fig. 1-10 A, B)[44]. The

rate of PCNA-positive hepatocytes was significantly increased at 48 h after PH (Fig. 1-10 B). These results suggest that PH stimulates the cell cycle and cell proliferation during liver regeneration in mice.

To evaluate hepatocyte mitosis during liver regeneration, I analyzed the hepatocyte mitotic index using H&E staining (Fig. 1-10C). The number of hepatocytes undergoing mitosis was dramatically increased in mice at 48 h after PH (Fig. 1-10D). The mitotic index was calculated by counting the number of nuclei in each phase of mitosis (prophase, metaphase, anaphase, and telophase) (see yellow arrow in Fig. 1-10C).

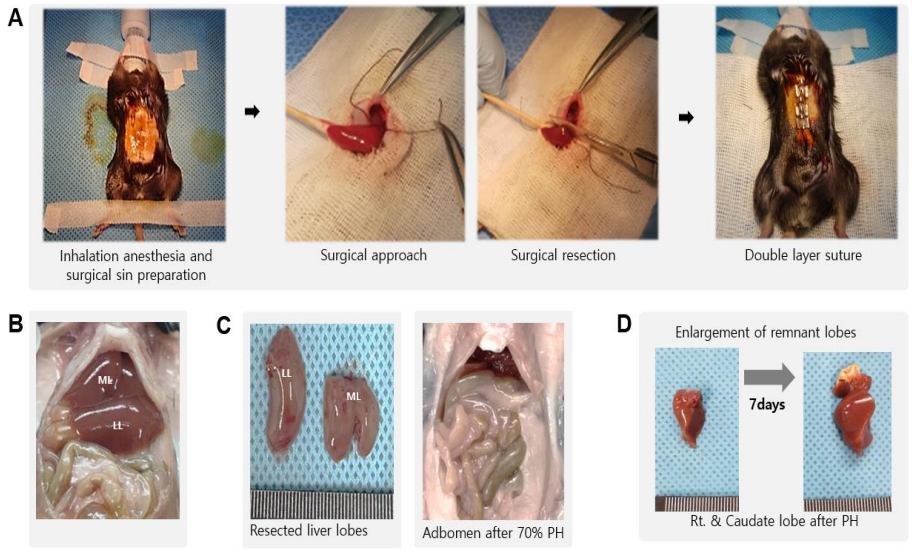

Figure 1-7. Surgical procedure and liver gross in mice

(A) Representative images of surgical procedure for 70% PH in C57BL/6 mice. (B) Representative image of the normal abdomen in C57BL/6 mice. (C) Representative image of resected liver lobes and abdomen after PH. (D) Representative images of remnant lobes promptly and 7days after PH.

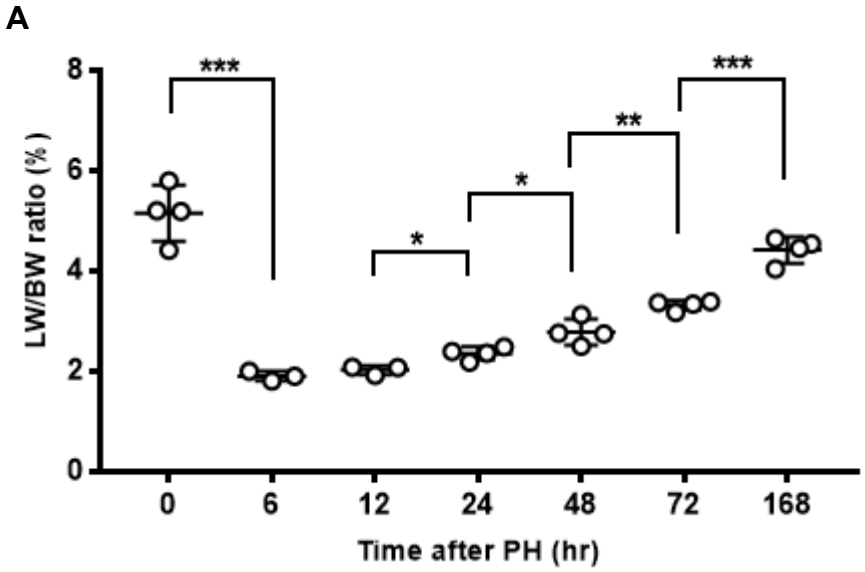

Figure 1-8. Liver regeneration rate for 7days after PH in mice

(A) Liver to body weight ratios at the indicated time points after PH in mice; n=4, per group. Values are shown as means ± SD. Significance calculated using unpaired two-tailed student's t-test. *p < 0.05, **p < 0.01, ***p < 0.001.

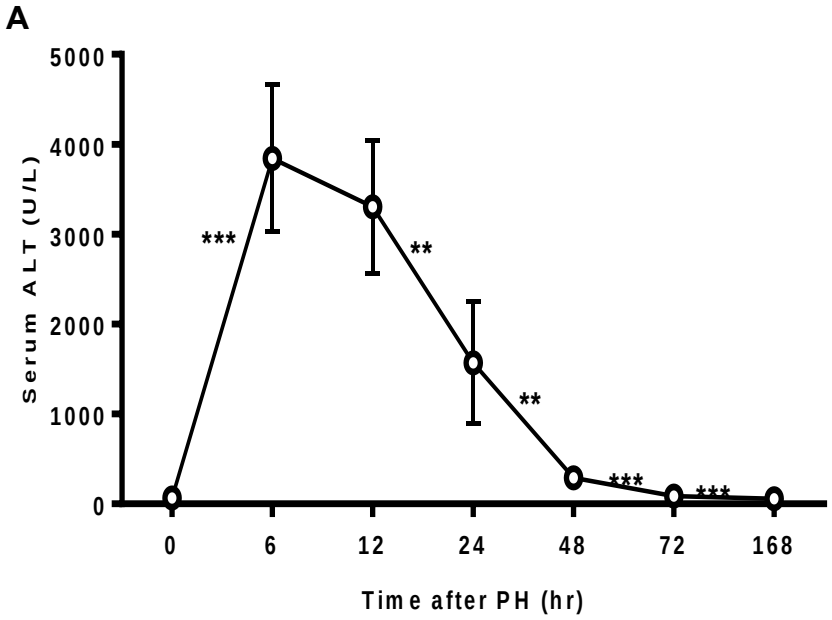
A
5000
4000
3000
2000
1000
0
Serum ALT (U/L)
***
**
**
***
***
0
6
12
24
48
72
168
Time after PH (hr)

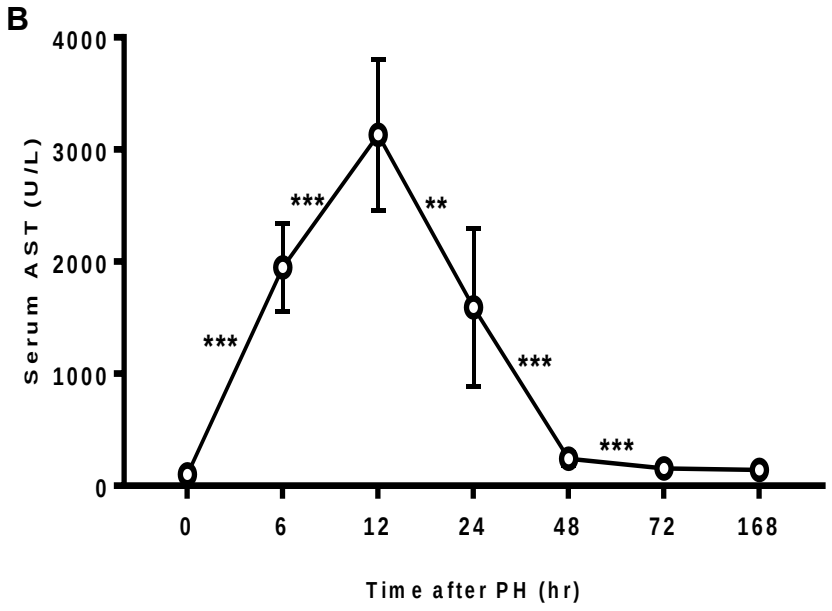
B
4000
3000
2000
1000
0
Serum AST (U/L)
***
***
**
***
***
0
6
12
24
48
72
168
Time after PH (hr)

Figure 1-9. Serum analysis for ensuring liver function after PH in mice

(A) Serum ALT at the indicated time points after PH in C57BL/6 mice; n=3, per group. (B) Serum AST at the indicated time points after PH in C57BL/6 mice; n=3, per group. Values are shown as means ± SD. Significance calculated using unpaired two-tailed student's t-test. *p < 0.05, **p < 0.01, ***p < 0.001.

A

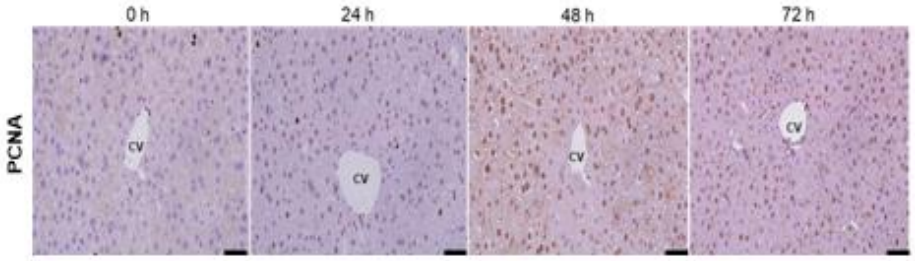
0 h
24 h
48 h
72 h
PCNA
cv
cv
cv
cv

B

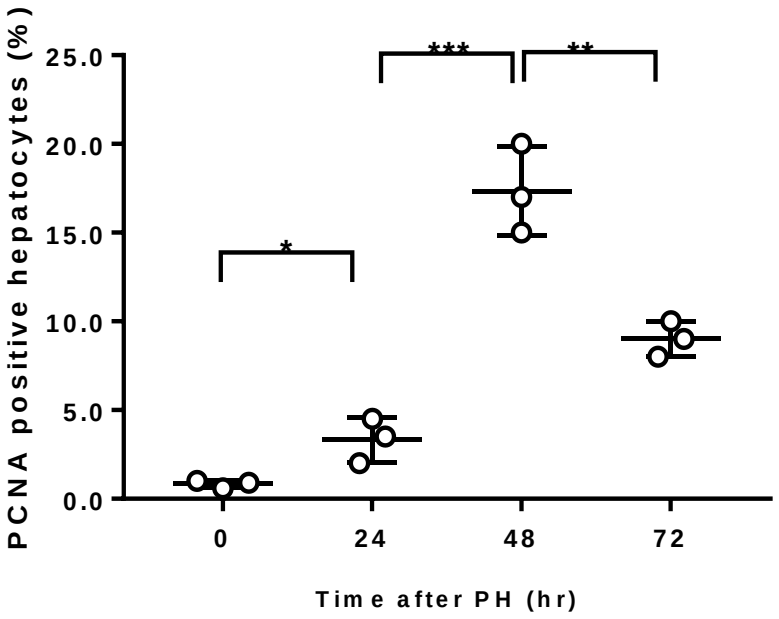
PCNA positive hepatocytes (%)
25.0
20.0
15.0
10.0
5.0
0.0
*
***
**
0
24
48
72
Time after PH (hr)

C

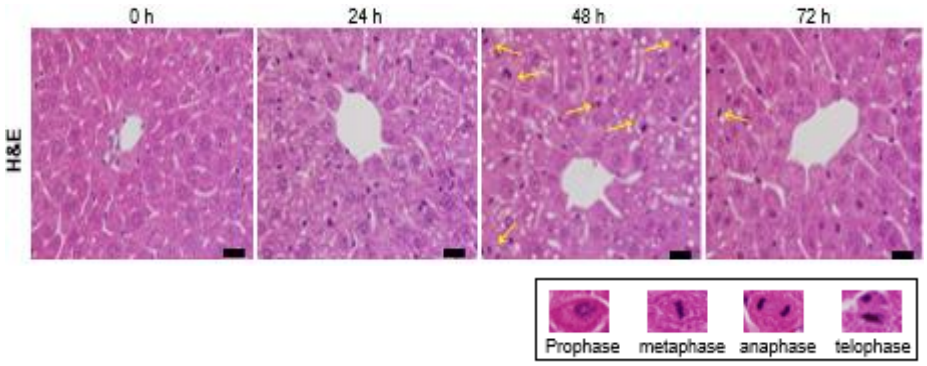
0 h
24 h
48 h
72 h
H&E
Prophase
metaphase
anaphase
telophase

D

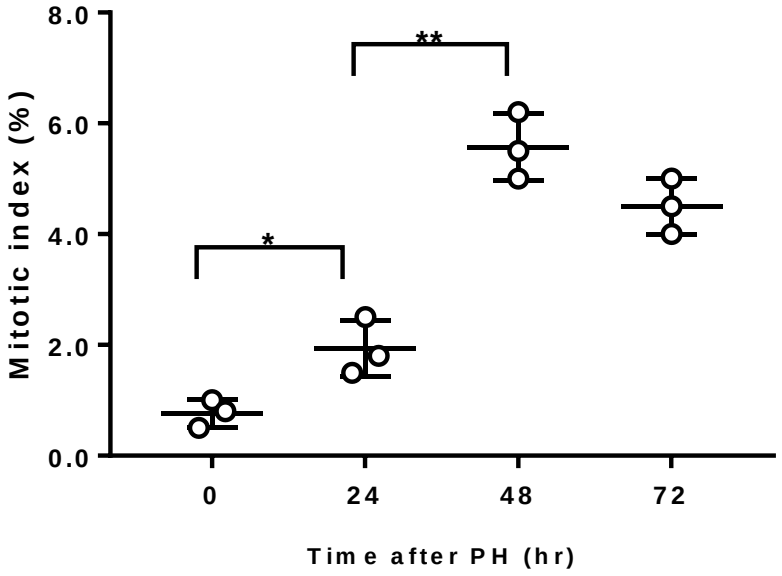
8.0
6.0
4.0
2.0
0.0
Mitotic index (%)
*
**
0
24
48
72
Time after PH (hr)

Figure 1-10. Hepatocyte proliferation in LR after PH in mice

(A) Representative immunostaining images showing proliferating cell nuclear antigen (PCNA) staining images in the liver after PH in C57BL/6 mice. Scale bar=50 μm. (B) Quantification of PCNA staining in hepatocyte nuclei at the indicated time points after PH; n=3, per group. (C) Hematoxylin-eosin (H&E) staining images in the liver after PH in C57BL/6 mice. Scale bar=10 μm. (D) Quantification of hepatocyte nuclei undergoing mitosis at the indicated time points after PH; n=3, per group. Values are shown as means ± SD. Significance calculated using unpaired two-tailed student's t-test. *p < 0.05, **p < 0.01, ***p < 0.001.

1.3.2. External and paracrine signals associated with liver regeneration

To confirm the effect of external and paracrine signals associated with liver regeneration following PH, I examined the expression of growth factors, such as HGF, EGF and IL-6. HGF and IL-6 are certain mitogens derived from non-parenchymal liver cells, leading to the initiation phase of liver regeneration[45,46]. In contrast, EGF is one of the complete mitogens secreted from the Brunner's gland of the duodenum[27,47]. HGF, EGF and IL-6 gene expression levels were gradually increased and then reversibly decreased to pre-surgery levels (Fig. 1-11A-C, Fig 1-13A).

To confirm the effect of PH on the cell cycle during liver regeneration, I examined the cell cycle-associated cyclin D1, E1, and B1 in C57BL/6 mice[48,49]. Cyclins are indicators of the regenerative activity of hepatocytes. Cyclin D1 plays a prominent role in proliferation and growth and is the most reliable marker for G1 progression in hepatocytes[50-52]. Cyclin A1 and B1 are associated with M phase[50,53]. Cyclin D1 expression was gradually increased and then reversibly decreased to pre-surgery levels

(Fig. 1-12C, Fig 1-13B). Cyclin B1 expression patterns were similar to that of cyclin D1 (Fig. 1-12B, Fig. 1-13B). Cyclin A1 gene expression was slightly increased in 72h after PH (Fig. 1-12A). Meanwhile, cyclin A2 protein expression was activated in early regenerative period after PH (Fig. 1-13B). The time-dependent changes in mRNA and protein expression levels during liver regeneration do not exactly overlap, the trends are similar.

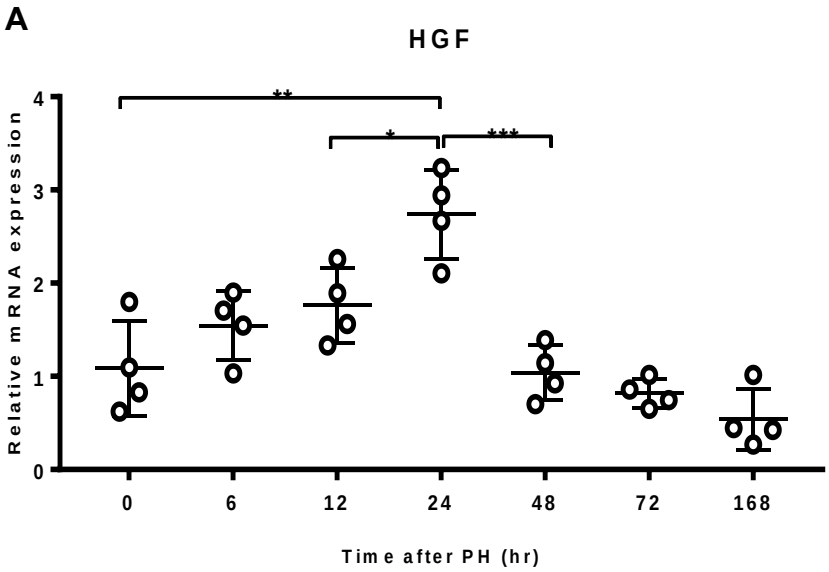
A
HGF
Relative mRNA expression
4
3
2
1
0
**
*
***
0
6
12
24
48
72
168
Time after PH (hr)

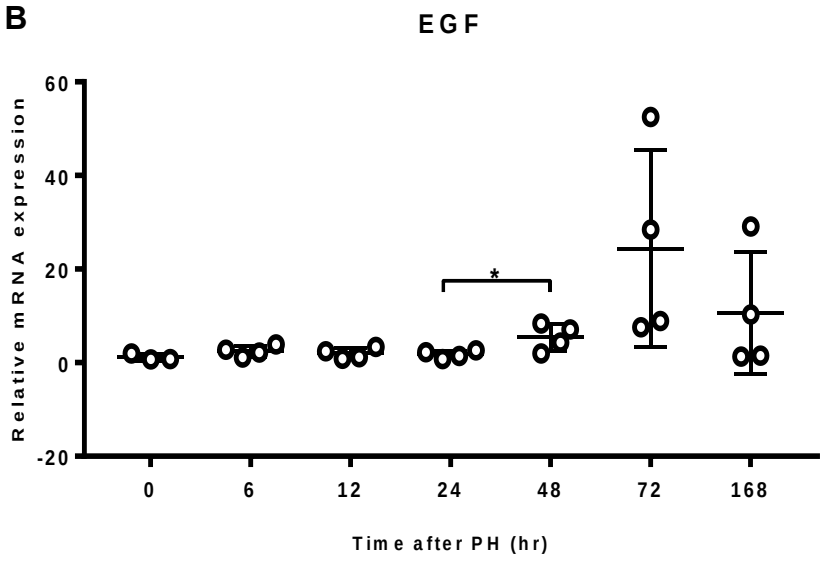
B
EGF
Relative mRNA expression
60
40
20
0
-20
*
0
6
12
24
48
72
168
Time after PH (hr)

C

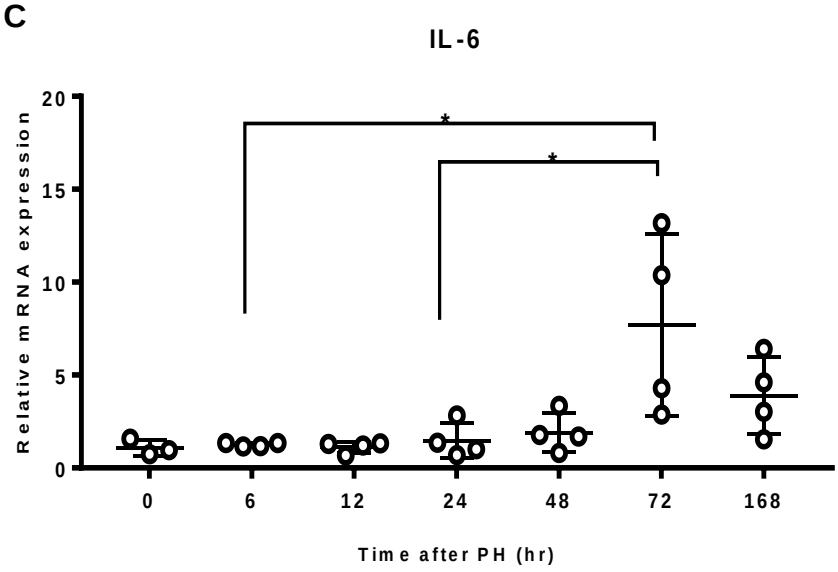
IL-6
Relative mRNA expression
20
15
10
5
0
*
*
0
6
12
24
48
72
168
Time after PH (hr)

Figure 1-11. LR initiative pathway-related gene expression in the liver after PH in mice.

(A) HGF mRNA expression levels in the liver at the indicated time points after PH in C57BL/6 mice; n=4, per group. (B) EGF mRNA expression levels in the liver at the indicated time points after PH in C57BL/6 mice; n=4, per group. (C) IL-6 mRNA expression levels in the liver at the indicated time points after PH in C57BL/6 mice; n=4, per group. Values are shown as means ± SD. Significance calculated using unpaired two-tailed student's t-test. *$p < 0.05$, **$p < 0.01$, ***$p < 0.001$.

A

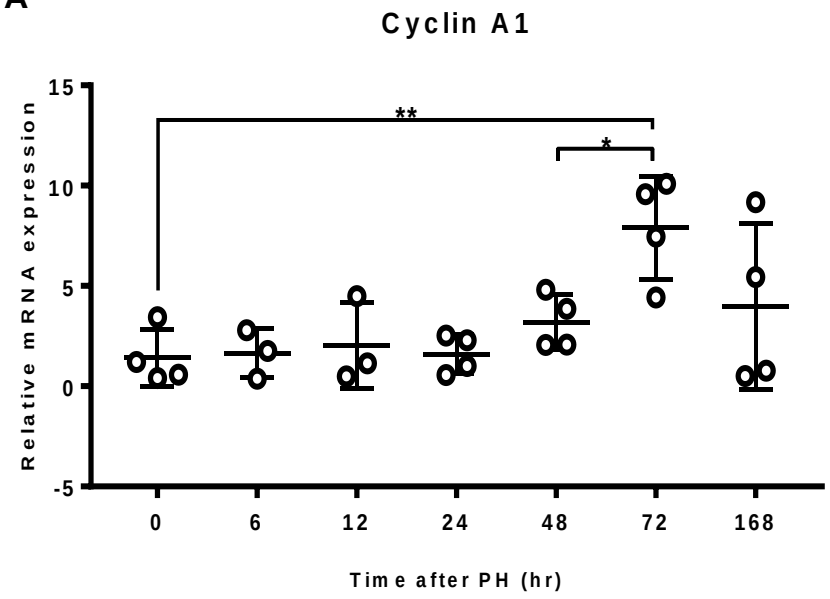
Cyclin A1
Relative mRNA expression
15
10
5
0
-5
**
*
0
6
12
24
48
72
168
Time after PH (hr)

B

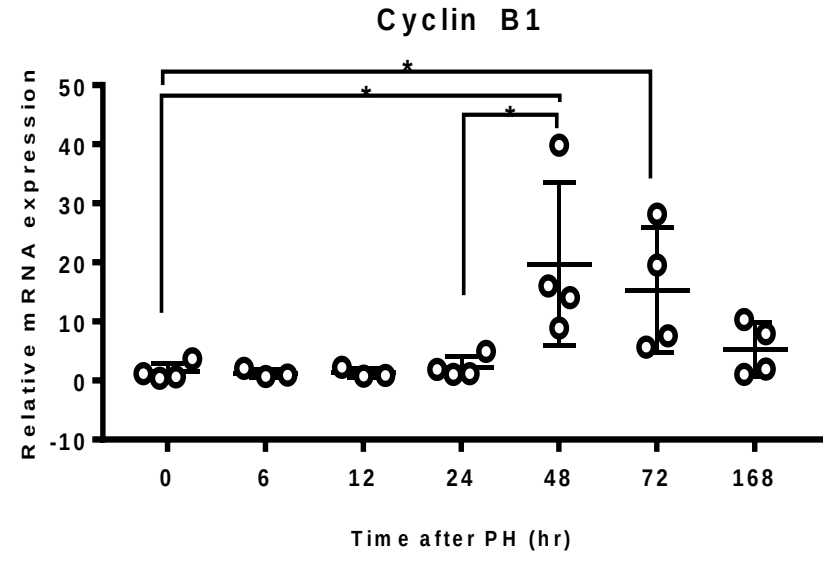
Cyclin B1
Relative mRNA expression
50
40
30
20
10
0
-10
*
*
*
0
6
12
24
48
72
168
Time after PH (hr)

C

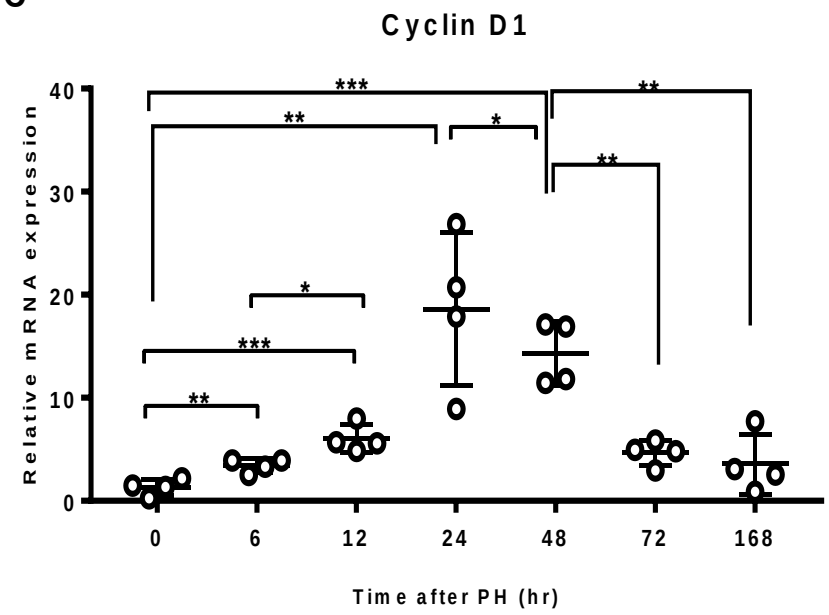
Cyclin D1
Relative mRNA expression
40
30
20
10
0
***
**
*
**
**
*
***
**
0
6
12
24
48
72
168
Time after PH (hr)

Figure 1-12. Cell cycle-related gene expression during LR after PH in mice

(A) Cyclin A1 expression levels in the liver at the indicated time points after PH in C57BL/6 mice; n=4, per group. (B) Cyclin B1 expression levels in the liver at the indicated time points after PH in C57BL/6 mice; n=4, per group. (C) Cyclin D1 expression levels in the liver at the indicated time points after PH in C57BL/6 mice; n=4, per group. Values are shown as means ± SD. Significance calculated using unpaired two-tailed student's t-test. *p < 0.05, **p < 0.01, ***p < 0.001.

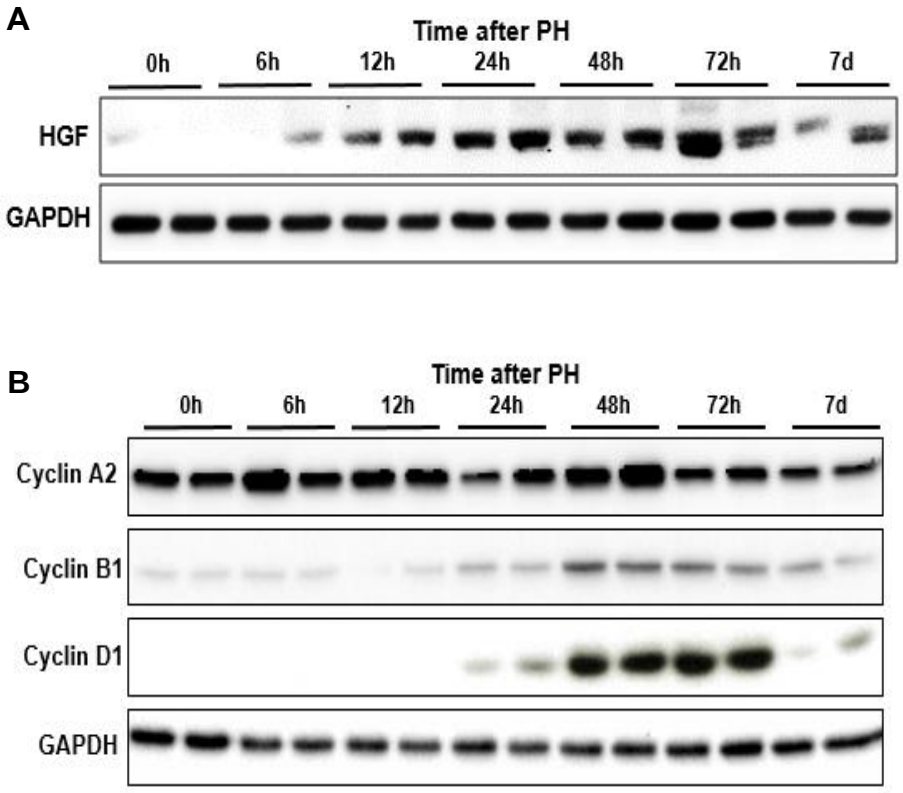
A
Time after PH
0h
6h
12h
24h
48h
72h
7d
HGF
GAPDH
B
Time after PH
0h
6h
12h
24h
48h
72h
7d
Cyclin A2
Cyclin B1
Cyclin D1
GAPDH

Figure 1-13. Cell cycle-related protein expression during LR after PH in mice

(A) Representative western blot of HGF in the liver at the indicated time points after PH in C57BL/6 mice. (B) Representative western blot of cyclin A2, cyclin B1 and cyclin D1 in the liver at the indicated time points after PH in C57BL/6 mice.

1-3-3. m^{6}A modification pathway influences liver regeneration in C57BL/6 mice following 70% PH

Next, I assessed the expression of the m^{6}A modification-related factors METTL3, METTL14, FTO, and YTHDF2[37]. Gene expression of *Mettl3* and *Ythdf2* increased from 24h after PH and then gradually decreased from 72h after PH (Fig. 1-14A, C). Meanwhile, gene expression of Mettl14 and *Fto* were not expressed consistently after PH (Fig. 1-14B, D). I examined the expression of m^{6}A modification-related proteins METTL3, METTL14 and YTHDF2. Expression of METTL3 and YTHDF2 increased from 24 h after PH and then gradually decreased from 72 h after PH (Fig. 1-15A). Expression of METTL14 was gradually increased from 48h to 7 days after PH (Fig. 1-15B, C).

To determine the role of the m^{6}A methyltransferases, *Mettl3* and *Mettl14*, I analyzed m^{6}A relative quantification in total RNA at 48h and 72h after PH. m^{6}A was significantly increased (Fig. 1-16). The global m^{6}A levels measured by m^{6}A colorimetric analysis were gradually increased during liver regeneration[14]. These findings are consistent with previous reports and suggest

that the m^6A modification pathway with METTL3 and METTL14 may influence liver regeneration after PH[15,16].

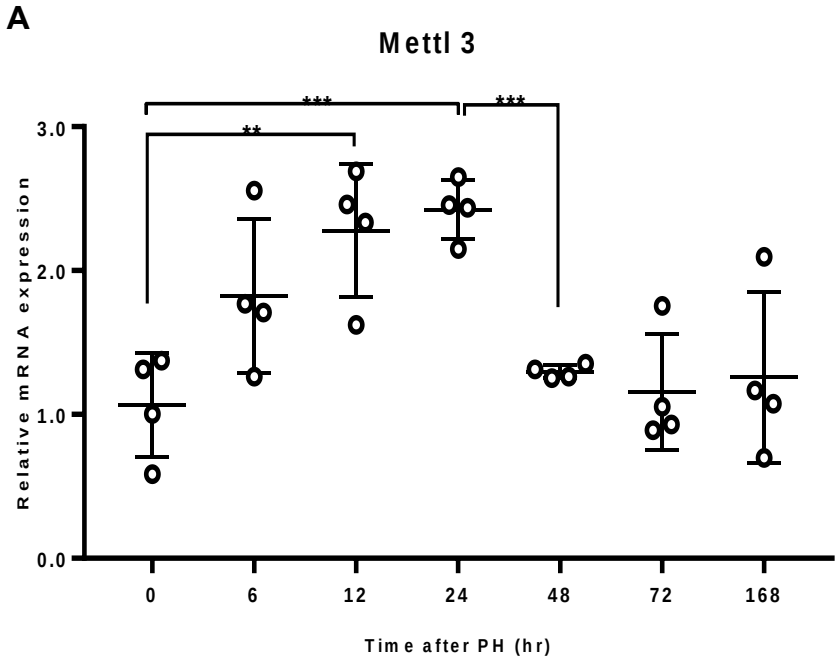
A
Mettl 3
***
***
**
3.0
2.0
1.0
0.0
Relative mRNA expression
0
6
12
24
48
72
168
Time after PH (hr)

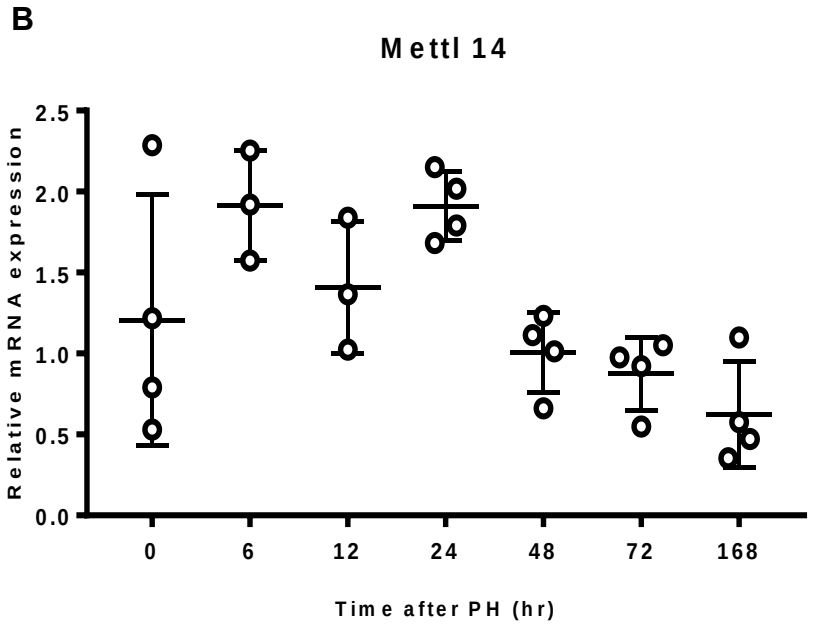
B
Mettl 14
2.5
2.0
1.5
1.0
0.5
0.0
Relative mRNA expression
0
6
12
24
48
72
168
Time after PH (hr)

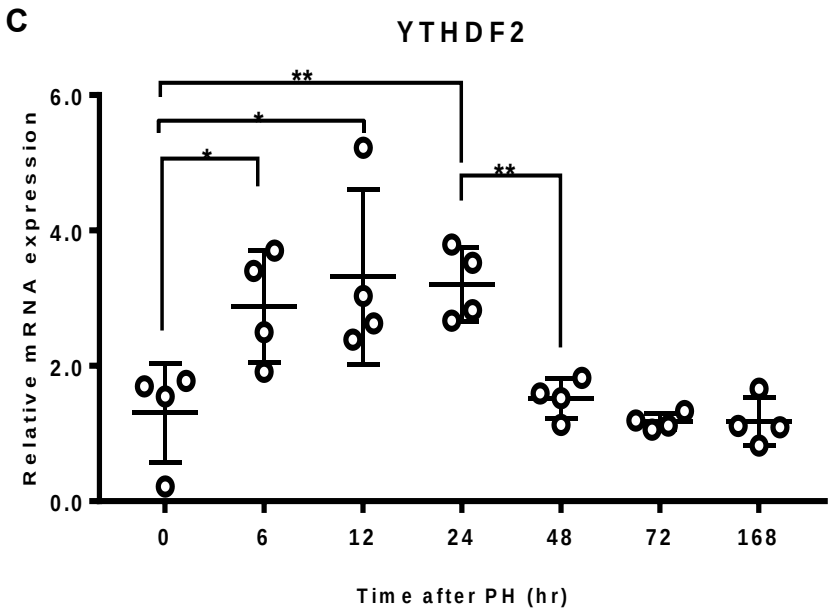
C
YTHDF2
Relative mRNA expression
6.0
4.0
2.0
0.0
**
*
*
**
0
6
12
24
48
72
168
Time after PH (hr)

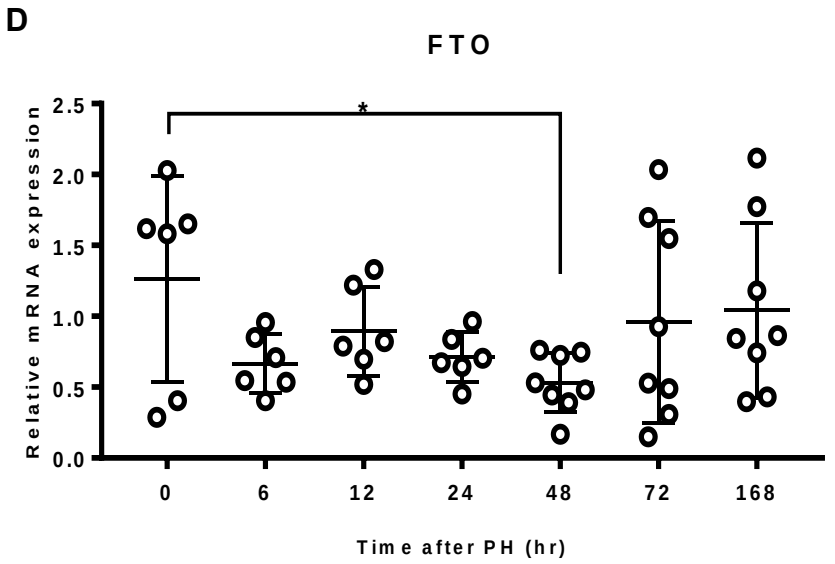
D
FTO
Relative mRNA expression
2.5
2.0
1.5
1.0
0.5
0.0
*
0
6
12
24
48
72
168
Time after PH (hr)

Figure 1-14. m^6A modification pathway-related gene expression in the liver after PH in mice

(A) Mettl3 mRNA expression in the liver after PH in mice; n=4, per group. (B) Mettl14 mRNA expression in the liver after PH in mice; n=4, per group. (C) YTHDF2 mRNA expression in the liver after PH in C57BL/6 mice; n=4, per group. (D) FTO mRNA expression in the liver after PH in C57BL/6 mice; n=4, per group. Values are shown as means ± SD. Significance calculated using unpaired two-tailed student's t-test. *p < 0.05, **p < 0.01, ***p < 0.001

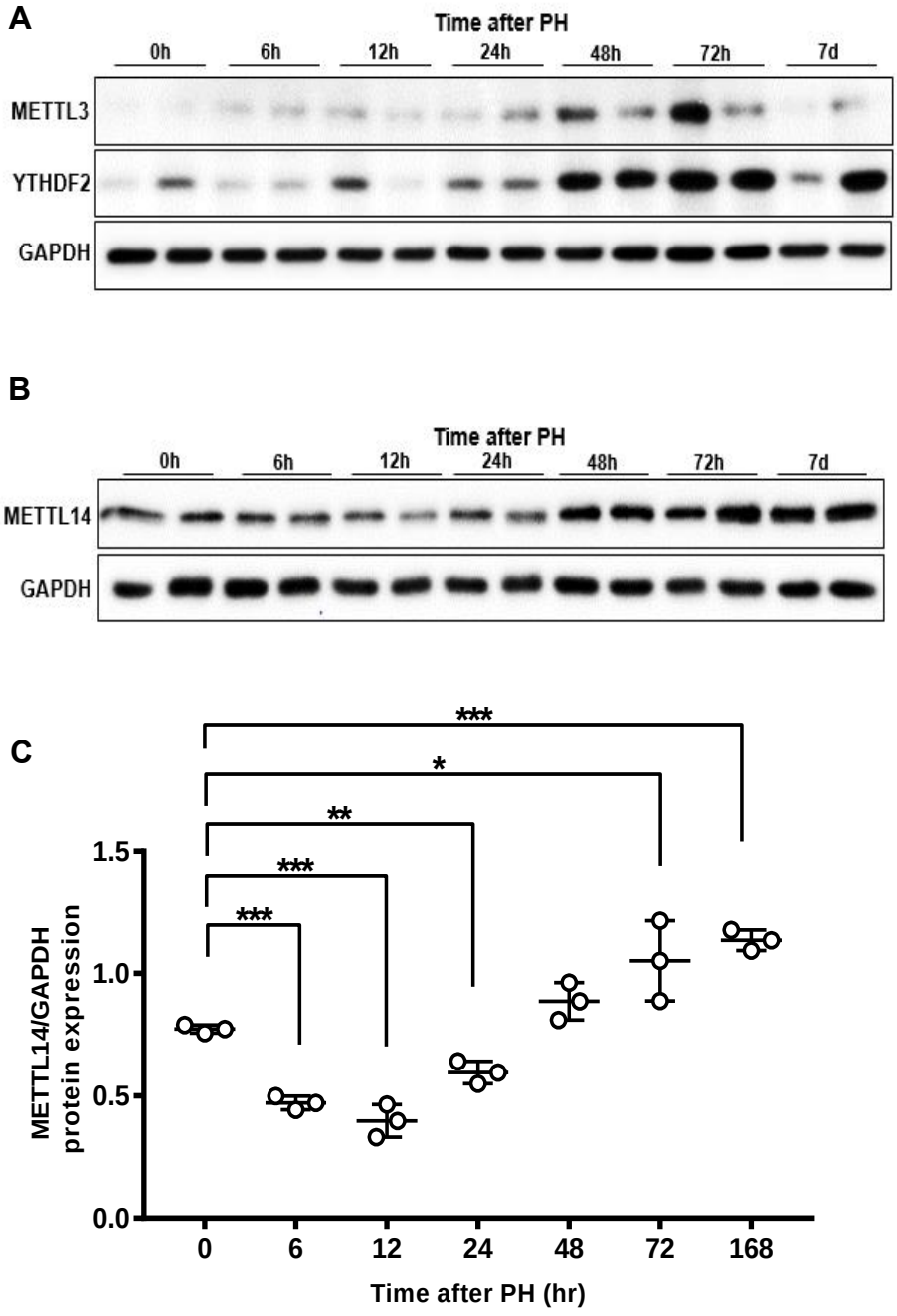
A
Time after PH
0h
6h
12h
24h
48h
72h
7d
METTL3
YTHDF2
GAPDH
B
Time after PH
0h
6h
12h
24h
48h
72h
7d
METTL14
GAPDH
C
***
*
**
***
***
1.5
1.0
0.5
0.0
METTL14/GAPDH protein expression
0
6
12
24
48
72
168
Time after PH (hr)

Figure 1-15. m6A modification pathway-related protein expression in LR after PH in mice

(A) Representative western blot of METTL3 and YTHDF2 in the liver at the indicated time points after PH in C57BL/6 mice. (B) Relative protein level of METTL14 in the liver at the indicated time points after PH in C57BL/6 mice; n=4, per group. (C) Representative western blot of METTL14 in the liver at the indicated time points after PH in C57BL/6 mice. Values are shown as means ± SD. Significance calculated using unpaired two-tailed student's t-test. *$p < 0.05$, **$p < 0.01$, ***$p < 0.001$

A

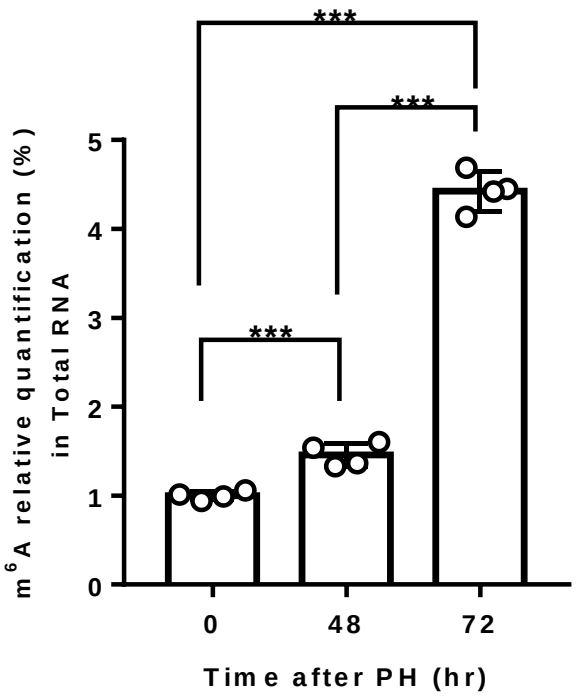
***
***
***
5
4
3
2
1
0
m6A relative quantification (%)
in Total RNA
0
48
72
Time after PH (hr)

Figure 1-16. m^6A quantification in the liver after PH in mice

(A) m^6A relative quantification ratio in total RNA in the liver after PH in C57BL/6 mice; n=4, per group. Values are shown as means ± SD. Significance calculated using unpaired two-tailed student's t-test. *p < 0.05, **p < 0.01, ***p < 0.001

1.4 Discussion

The liver is the only organ with regenerative ability, and the liver-to-body weight ratio is maintained at the required level (100%) for homeostasis[17,32]. To study this crucial regenerative ability, a 70% partial hepatectomy (PH) has been widely used as a model of acute liver damage. This model has been used to reveal the extracellular and intracellular signaling mechanisms involved in the process of restoring the liver to its pre-surgery size and weight[17,30].

Several pathways related to liver regeneration have revealed. However, the detailed mechanisms have not yet been determined[17,40]. In particular, m^6A modification pathway in liver regeneration is not well understood. First, I observed that the ratios of liver to body weight was higher at indicated time after PH, and I analyzed the hepatocyte proliferation rate using PCNA-positive hepatocytes, which was significantly increased at indicated time after PH[30,44]. It consistent with the results of the liver weight-to-body weight ratio.

Next, I analyzed the mRNA expression pattern of HGF, EGF and IL-6 after PH in C57BL/6 mice, which showed that expression gradually increased and then reversibly decreased to pre-surgery levels, and these genes are well known to regulate liver regeneration. Expression of cyclin A1, A2, B1 and D1, which regulates cell-cycle, were also gradually increased, and then reversibly decreased. In addition, I observed that the expression of Mettl3, Mettl14 and YTHDF2, which regulates m6A modification pathway. The expression of Mettl3, Mettl14 and YTHDF2 were also gradually increased and then reversibly decreased to pre-surgery levels, and these patterns were similar to those of genes that regulate liver regeneration, suggesting that Mettl3, Mettl14 and YTHDF2, which are m^6A modification factors, may regulate liver regeneration[31].

Finally, I observed relative m^6A quantification in the liver tissue, it was increased at indicated time after PH. These results show that m^6A modification pathway promotes liver regeneration. Although some inconsistency between the experimental groups was observed, the degree of expression was evaluated based on the trend in the regenerative process.

This suggests that liver regeneration affected by m^6A modification. Therefore, further research is needed to validate my findings.

Chapter Ⅱ

Understanding the Role of m^6A Modification in Liver Regeneration after Partial Hepatectomy in Mice

2.1 Introduction

N6-methyladenosine (m^6A) is the most common intrinsic RNA modification of eukaryotic cells, and is the most prevalent, abundant, and conserved internal transcriptional modification in eukaryotic cells[2,54,55]. m^6A modification was discovered in the 1970s and has obtained interest as a new layer of control for gene expression[1]. The discovery of m^6A methyltransferases and demethylases suggests that m^6A modification pathway is a dynamic process[1].

Recently, it reported that the m^6A modification pathway has been associated with hepatocellular carcinoma and liver regeneration[1,2,13-16]. It has been proven to affect liver regeneration in mice lacking hepatocyte-specific m^6A methyltransferase (Fig. 2-1)[16]. But, its precise role in the initiation phase of liver regeneration that is influenced by endothelial cells, stellate cells, and Kupffer cells, which act as regenerative stimulators, remains to be elucidated[15,16,33].

In mammals, hepatocytes play most of the hepatic functions related to body homeostasis and take for more than 80% of liver

mass[27,31,32,56]. And, all hepatic cell types involve in cell proliferation during liver regeneration after PH, but stem cells are not participated (Fig 2-2)[30,57]. Some of the earliest events after PH occur in hepatocytes.

Hepatocyte proliferation during liver regeneration is controlled by multiple extracellular signals, like MET and EGFR, these play directly mitogenic effect in liver regeneration[25,30]. Moreover, Intracellular signaling pathways in hepatocytes are very rapidly activated within minutes after PH[24,58,59]. The mechanisms triggering these pathways are not understood.

In this study, I generated global *Mettl14* knockout mice to evaluate METTL14-related m^6A modification to the non-parenchymal mitogenic pathway in liver regeneration after PH[30].

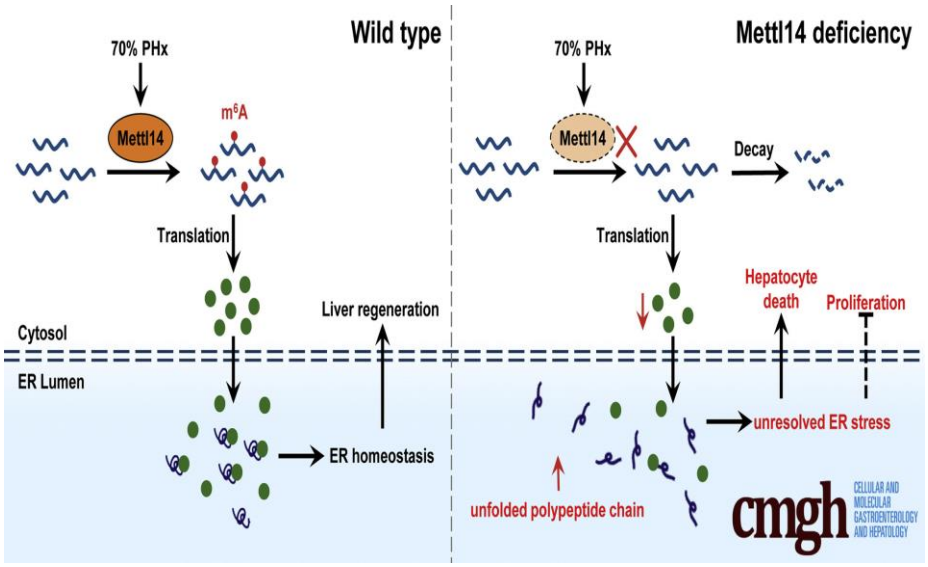

Figure 2-1. Mettl14-Mediated m6A Modification Facilitates Liver Re-generation by Maintaining Endoplasmic Reticulum Homeostasis (Cao X, Cell Mol Gastroenterol Hepatol, 2021).

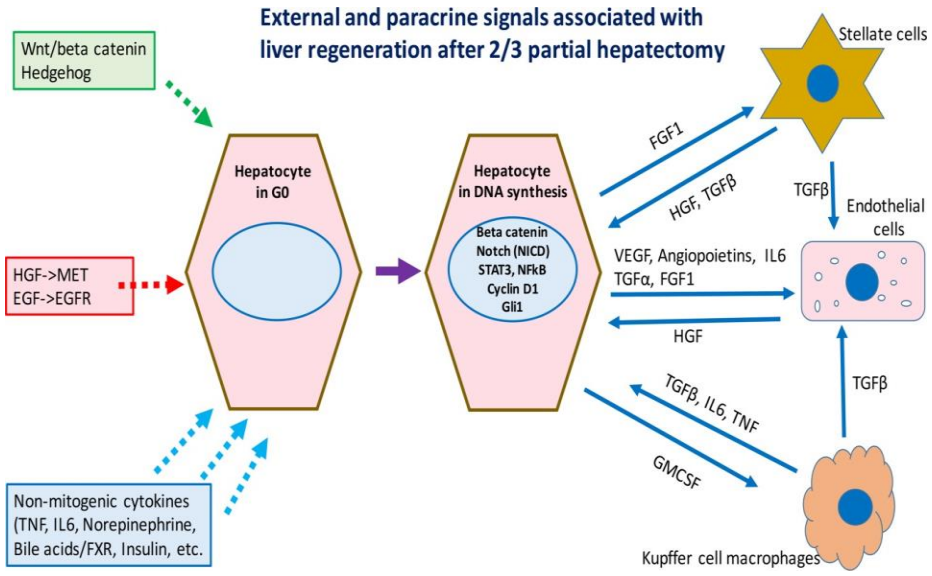

Figure 2−2. External and paracrine signals associated with liver regeneration after 2/3 partial hepatectomy (Michalopoulos GK, Hepatology, 2017).

2.2 Materials and Methods

Animals

Mice were maintained under a 12-h light-dark cycle and were provided with free access to water and a regular chow diet in a specific pathogen-free (SPF) facility.

The C57BL/6N-Mettl14<em1(IMPC)Tcp> mice were produced as part of the KOMP2-Phase2project at the Center for Phenogenomics of International Mouse Phenotyping Consortium (IMPC) and were obtained from the Canadian Mouse Mutant Repository. According to IMPC data, Homozygous offspring of *Mettl14* knockout mice exhibited preweaning or embryonic lethality.

The *Mettl14* HET mice and WT mice were created by the deletion of *Mettl14*; endonuclease-mediated 1 allele, as published by the IMPC. Genotyping was performed using genomic DNA desolated from tails according to the IMPC screening protocol.

Partial hepatectomy

Male mice, aged 8 to 10 weeks, were subjected to 70% partial hepatectomy under isoflurane (Hana Pharm Co., Ltd.) inhalation anesthesia according to a published protocol[28,29,41].

The left lateral and median lobe of the liver along with the gall bladder were ligated and removed. The gall bladder was always removed during surgery to avoid damage. For postoperative care, all animals were administrated 5mg/kg ketoprofen (Daehan Inc., Korea) intraperitoneally to control pain[41]. All mice were sacrificed at the indicated time. The weight of the remnant livers was measured, which were then subsequently fixed in 4% paraformaldehyde and snap-frozen in liquid nitrogen immediately after extraction. Animal experiments were performed following the "Guide for Animal Experiments" edited by the Korean Academy of Medical Sciences and "ARRIVE Guidelines" by NC3Rs and approved by the Institutional Animal Care and Use Committee of Seoul National University, Seoul, Korea (IACUC approval no. SNU-210709-4).

Histology and Immunohistochemistry

Liver tissues were fixed overnight in 4% paraformaldehyde, embedded in paraffin, and used for hematoxylin and eosin (H&E) staining, as well as immunostaining with antibodies against MKI67 (cat. ab16667; Abcam, Cambridge, UK). For immunostaining, the slides containing tissue sections were first heated in citrate buffer for antigen retrieval before being treated with horse serum for blocking the endogenous peroxidase activity. Slides were then incubated with the primary antibody overnight, followed by a 30min incubation with the secondary antibody (horse Anti Rabbit HRP). The slides were then developed with diaminobenzidine (DAB). To quantify hepatocyte proliferation, ten fields per slide were randomly chosen under the microscope after immunostaining to count MKI67-positive hepatocytes and the percentage of MKI67-positive hepatocytes was calculated against the total hepatocytes in the fields.

Western blotting

Protein lysates were prepared in RIPA buffer containing 0.5 mM phenylmethane sulfonyl fluoride (PMSF), 4 μg/ml leupeptin,

4 μg/ml aprotinin, and 4 μg/ml pepstatin, separated by sodium dodecyl sulfate (SDS)-polyacrylamide gel electrophoresis (PAGE), and transferred to polyvinylidene fluoride (PVDF) membranes. Membranes were incubated with the following primary antibodies overnight: METTL3 (cat. 96391, Cell Signaling Technology, MA, USA), METTL14 (cat. HAP038002; Sigma-Aldrich, MO, USA), YTHDF2 (cat. ab220163), TNF-α (cat. 11948, Cell Signaling Technology), HGF (cat. ab83760), EGFR (cat. 2646; Cell Signaling Technology), Cyclin B1 (cat. 12231; Cell Signaling Technology), Cyclin D1(cat. 2978; Cell Signaling Technology), CDK4 (cat. Sc-23896; Santa Cruz Biotechnology, Inc., USA), GAPDH (cat. 2118, Cell Signaling Technology) then incubated with the secondary antibody goat-anti-rabbit-HRP or goat-anti-mouse-HRP for 1h. Antibody binding was visualized using the Pierce TM ECL western blotting detection system (Chemi-Doc XRS+System; Bio-rad, CA, USA).

mRNA isolation and real-time polymerase chain reaction (RT-PCR)

Total RNA was isolated from the liver using Trizol (Ambion, TX, USA) reagent. RT-PCR analysis of the isolated mRNA was performed in a two-step reaction [43]. In the first step, a complementary DNA strand was synthesized using the Acculower RT reverse transcription kit (Bioneer, Daejeon, South Korea), and the second step was performed on a 7500 Real-Time PCR System (Applied Biosystems, MA, USA) with SYBR green (BIO-94020; Bioline, Toronto, Canada) and specific primers for each of the target genes. Each assay included the *36B4* gene as an endogenous reference. Gene expression was calculated using the $2^{-\triangle\triangle CT}$ method.

Analysis of Bulk-RNA sequencing and bioinformatics work

llumina's TruSeq Stranded mRNA LT Sample Prep Kit was used to prepare RNA-Sequencing libraries and high-throughput sequencing was performed with llumina's NovaSeq 6000 Platform for each sample. Adapter sequences and low-quality reads were removed with Trimmomatic v0.38. Sequenced reads after quality control were mapped to GRCm39 mouse reference genome using HISAT2 v2.1.0 and Bowtie2 2.3.4.1. Transcripts

were assembled and quantified with StringTie v.2.1.3. Differential expression analysis was performed using R package DESeq2 v.1.38.3 and ashr v2.2.54 as a shrinkage method. Differentially expressed genes were identified with cutoff of adjusted-P value < 0.05 and absolute value of log2 fold change > 0.58. Graphical Visualization was done with ggplot2 v3.4.2 and ComplexHeatmap v2.14.0

Statistical analysis

Statistical analysis was performed using Graph Pad Prism 7.0 (Graph Pad Software, La Jolla, CA, USA). Data are presented as mean ± standard deviation (SD). Statistical significance among more than two groups was assessed using Student's t-test. A P-value less than 0.05 was considered statistically significant.

2.3 Results

2.3.1. *Mettl14* depletion attenuates the initiative pathway of liver regeneration after PH in mice

These results suggested that *Mettl14* is more significantly expressed during liver regeneration after PH; therefore, to validate the effect of METTL14 in the initial pathway of liver regeneration after PH, I produced *Mettl14* knockout mice. To confirm the effect of METTL14 in liver regeneration, I performed 70% PH in *Mettl14* HET mice instead of homozygous mice, which have an embryo-lethal effect, and WT mice (Fig. 2-3A, B).

First, I evaluated the regenerative ability of the liver by calculating the ratio of liver weight to body weight for 72 h after PH. Although hepatic parenchymal proliferation after PH persists for 7 days, I focused on the initiative pathway and cell cycle-related factors[32]. The weight ratio was significantly higher in WT mice than in HET mice from 24 h to 72 h after PH (Fig. 2-4A). The level of alanine aminotransferase (ALT), a biomarker of liver function, was increased 48 h after PH and recovered close

to the pre-surgical level at 72 h after PH in both mice (Fig. 2-4B).

Next, I analyzed the liver regeneration initiative factors, such as HGF, which is a complete growth factor, and TNF-α, which is a cytokine. The mRNA expressions of both HGF and TNF-α were higher in WT mice than in HET mice before surgery and at 72 h after PH (Fig. 2-5A, B).

Furthermore, protein expressions of HGF and TNF-α were reduced at indicated time points after PH in HET mice compared to the WT mice (Fig. 2-6A). Meanwhile, protein expression of EGFR, which is mainly involved in liver regeneration, was increased in HET mice compared to WT mice at 24 h after PH (Fig. 2-6A)[37].

A

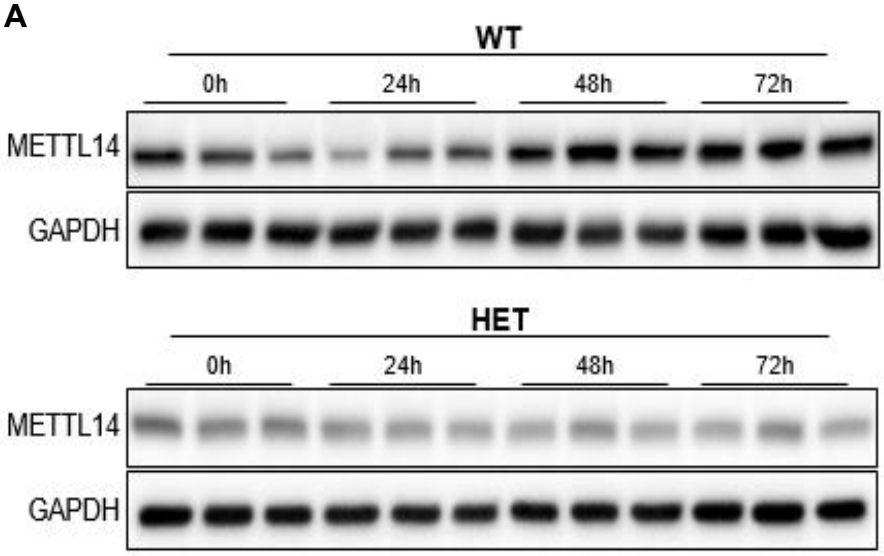
WT
0h
24h
48h
72h
METTL14
GAPDH
HET
0h
24h
48h
72h
METTL14
GAPDH

B

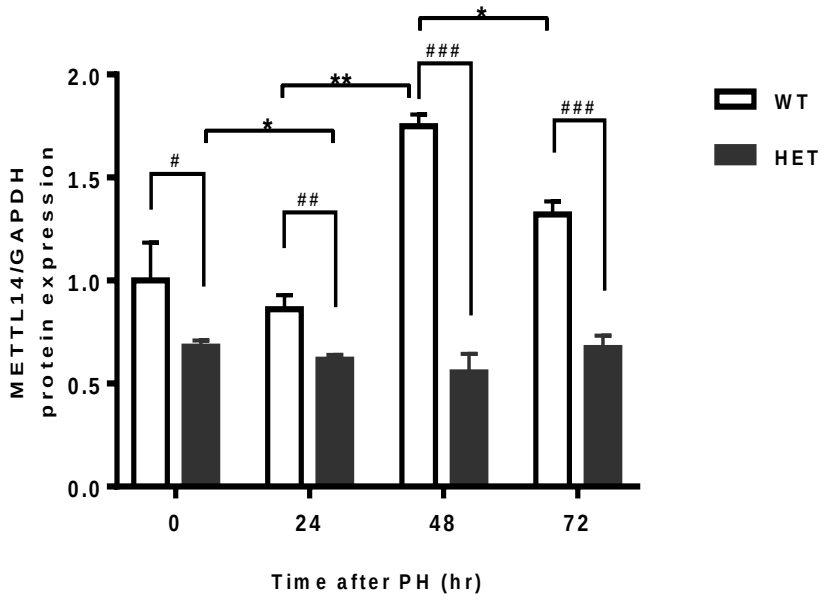
METTL14/GAPDH protein expression
2.0
1.5
1.0
0.5
0.0
0
24
48
72
Time after PH (hr)
WT
HET
*
**
*
#
##
###
###

Figure 2-3. METTL14 protein expression after PH in mice

(A) Representative western blot of METTL14 in the liver after PH in WT and HET mice; n=3, per group. (B) Relative protein level of METTL14 in the liver at the indicated time points after PH in WT and HET mice; n=3, per group. Values are shown as means ± SD. Significance calculated using unpaired two-tailed student's t-test. *P<0.05, **P<0.01 and ***P<0.001 when compared among time points in same group; #P<0.05, ##P<0.01 and ###P<0.001 when compared between WT and HET mice.

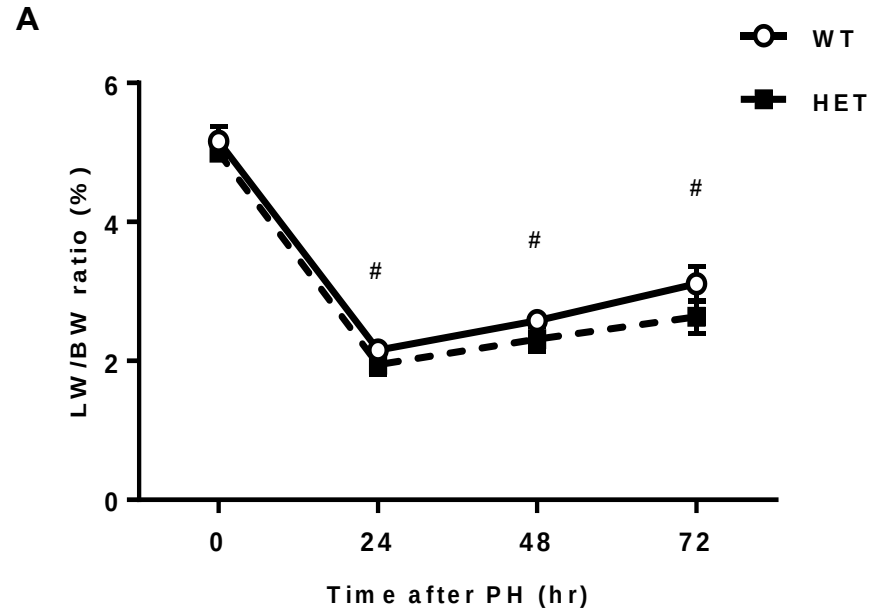
A
WT
HET
LW/BW ratio (%)
6
4
2
0
#
#
#
0
24
48
72
Time after PH (hr)

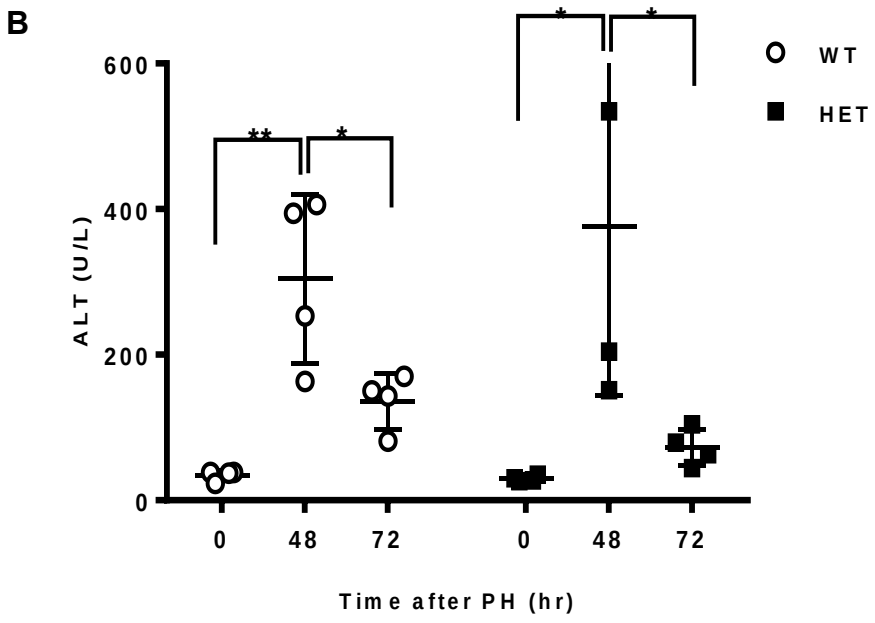
B
WT
HET
ALT (U/L)
600
400
200
0
**
*
*
*
0
48
72
0
48
72
Time after PH (hr)

Figure 2-4. *Mettl14* depletion restrains liver regeneration after PH

(A) Liver to body weight ratios at the indicated time points after PH in WT and HET mice; n=4, per group. (B) Serum ALT at the indicated time points after PH in WT and HET mice; n=4, per group. Values are shown as means ± SD. Significance calculated using unpaired two-tailed student's t-test. *P<0.05, **P<0.01 and ***P<0.001 when compared among time points in same group; #P<0.05, ##P<0.01 and ###P<0.001 when compared between WT and HET mice.

A

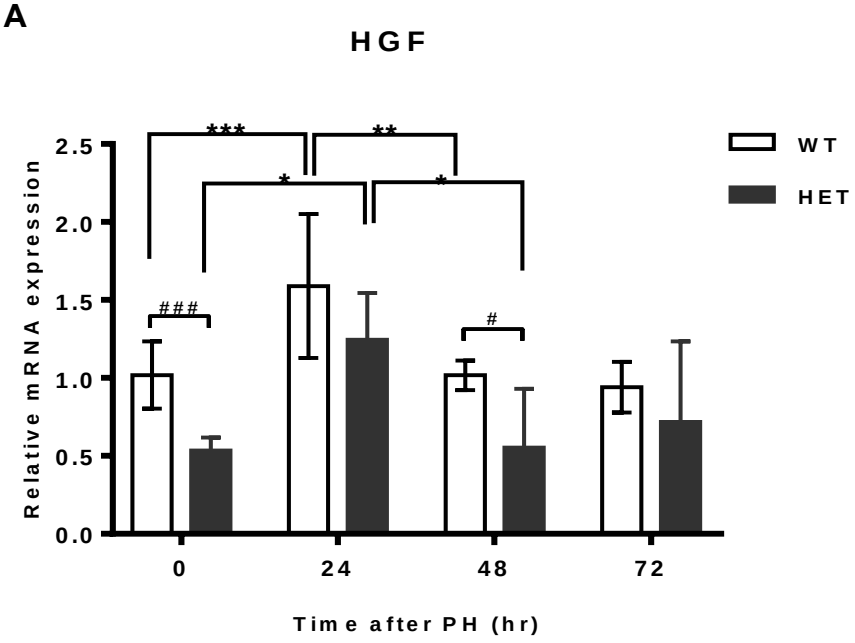
HGF
Relative mRNA expression
2.5
2.0
1.5
1.0
0.5
0.0
***
**
*
*
###
#
WT
HET
0
24
48
72
Time after PH (hr)

B

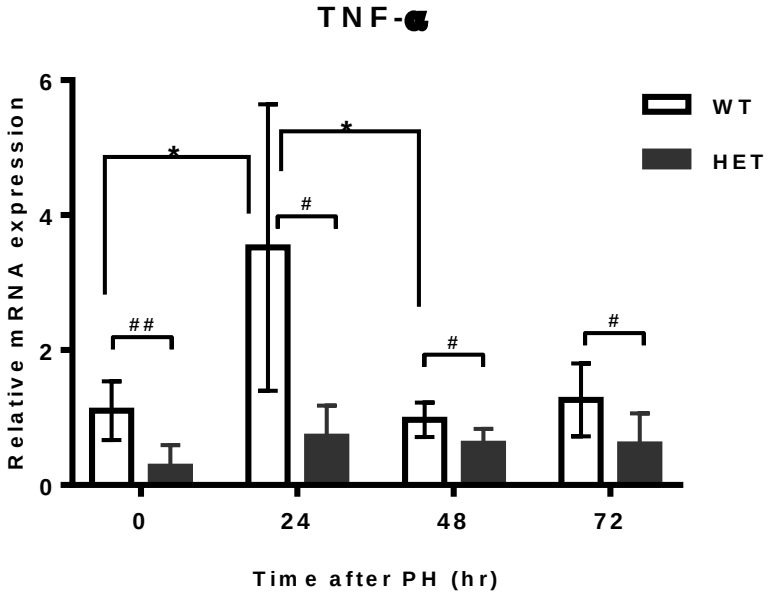
TNF-α
Relative mRNA expression
6
4
2
0
*
*
#
##
#
#
WT
HET
0
24
48
72
Time after PH (hr)

Figure 2-5. METTL14 depletion attenuates the LR initiative pathway-related gene expression in the liver after PH in mice.

(A, B) HGF and TNF-α mRNA expression levels in the liver at the indicated time points after PH in WT and HET mice (n = 4, each). Values are shown as means ± SD. Significance calculated using unpaired two-tailed student's t-test. *P<0.05, **P<0.01 and ***P<0.001 when compared among time points in same group; #P<0.05, ##P<0.01 and ###P<0.001 when compared between WT and HET mice.

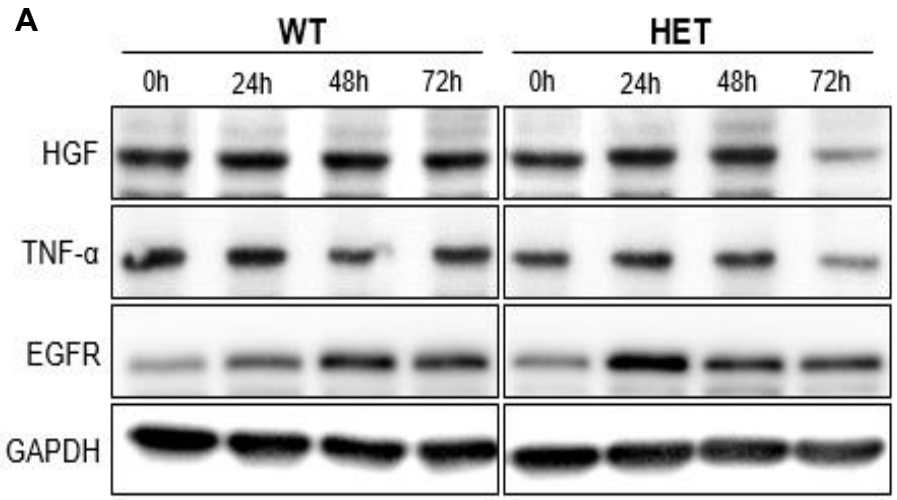

Figure 2-6. METTL14 depletion downregulates LR initiative pathway-related protein expression in the liver after PH in mice.

(A) Representative western blot of HGF, TNF-α and EGFR in the liver after PH in WT and HET mice

2.3.2. Mettl14 depletion downregulates cell cycle progression and reduces hepatocyte proliferation

To evaluate the effect of Mettl14 on the cell cycle progression during liver regeneration after PH, I studied the cell cycle-related cyclins B1 and D1, and CDK4[48-52]. Cyclin D1 plays an important factor in growth and proliferation and is the most reliable marker for G1 phase progression in liver regeneration[50,52]. CDK4 is a cyclin-dependent kinase and the main regulator of the cell cycle; it can combine with cyclin D1[49]. Cyclin B1 is related to the M phase[50]. The mRNA and protein expression of cyclin B1 and cyclin D1 at 24-72h after PH were higher in WT mice than in HET mice (Fig. 2-7, Fig. 2-8). However, CDK4 protein expression was not consistent with that of cyclin D1 (Fig 2-8A, B). As shown in Fig. 2-8, although the time-dependent results in mRNA and protein expression levels during liver regeneration did not follow the same pattern, there were similarities in the trends that increased and gradually decreased.

Next, I analyzed the hepatocyte proliferation rate using immunostaining of MKI67, which is more abundant in DNA synthesis and mitosis than in the early or even the very late G1 phase, as an indicator of cell cycle progression[60]. The proliferation rate was calculated by the number of stained nuclei (Fig. 2-9A). The rate of MKI67-positive hepatocytes was significantly increased in WT mice than in HET mice at 48 h and 72 h after PH (Fig. 2-9B).

A

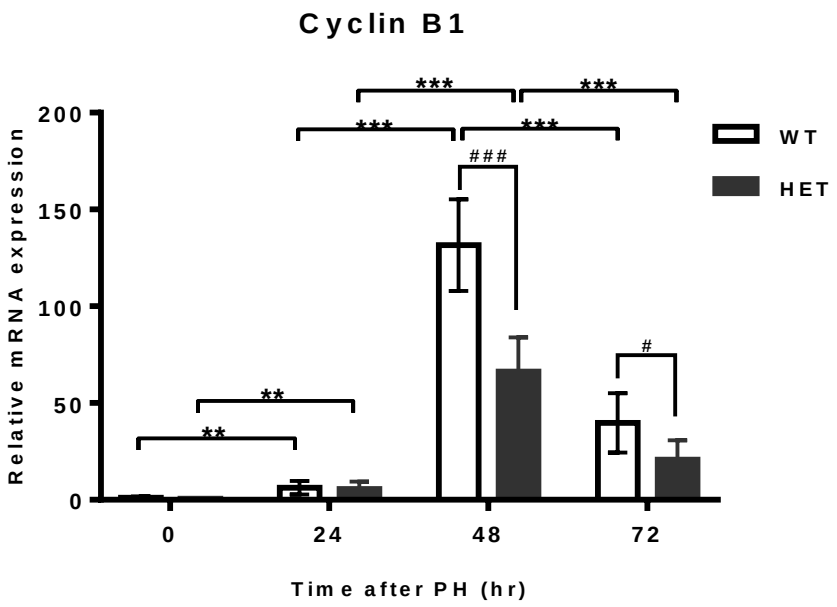
Cyclin B1
Relative mRNA expression
200
150
100
50
0
0
24
48
72
Time after PH (hr)
WT
HET
***
***
***
***
###
**
**
#

B

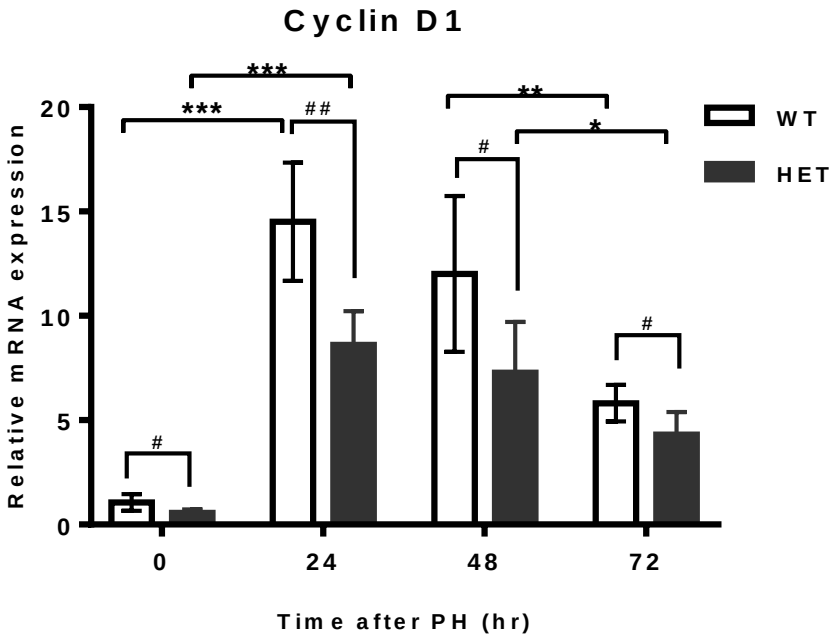
Cyclin D1
Relative mRNA expression
20
15
10
5
0
0
24
48
72
Time after PH (hr)
WT
HET
***
***
##
**
*
#
#
#

Figure 2-7. METTL14 depletion attenuates Cell cycle-related gene expression in the liver after PH in mice.

(A) Cyclin B1 mRNA expression in the liver after PH in WT and HET mice; n=4, per group. (B) Cyclin D1 mRNA expression in the liver after PH in WT and HET mice; n=4, per group. Values are shown as means ± SD. Significance calculated using unpaired two-tailed student's t-test. *P<0.05, **P<0.01 and ***P<0.001 when compared among time points in same group; #P<0.05, ##P<0.01 and ###P<0.001 when compared between WT and HET mice.

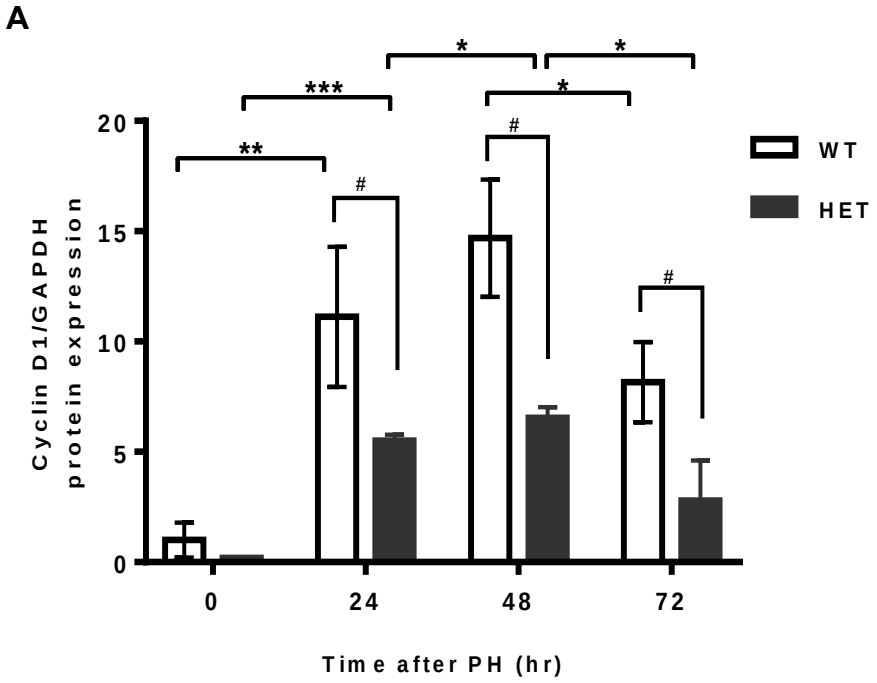
A
Cyclin D1/GAPDH protein expression
20
15
10
5
0
0
24
48
72
Time after PH (hr)
WT
HET
*
*
*
***
**
#
#
#

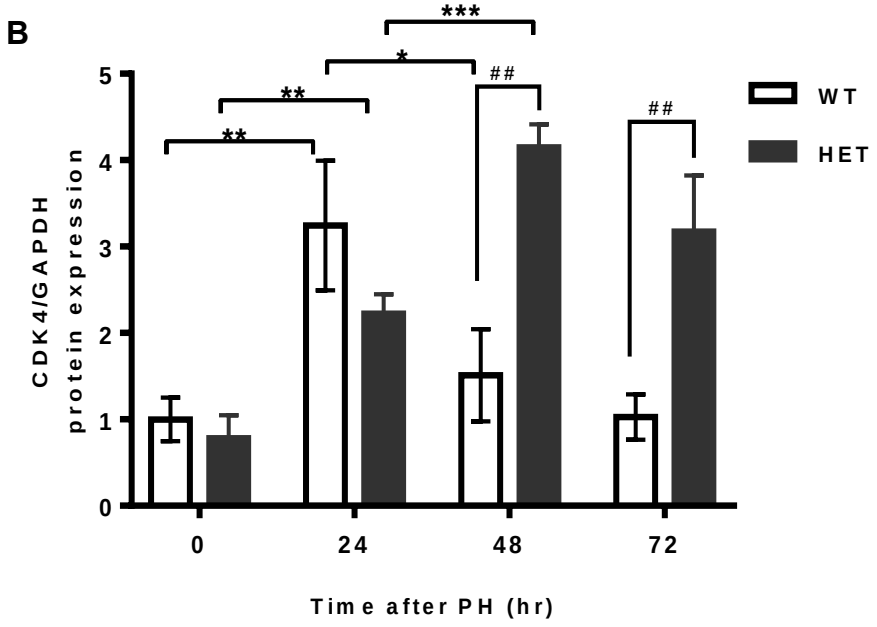
B
CDK4/GAPDH protein expression
5
4
3
2
1
0
0
24
48
72
Time after PH (hr)
WT
HET
***
*
**
**
##
##

C

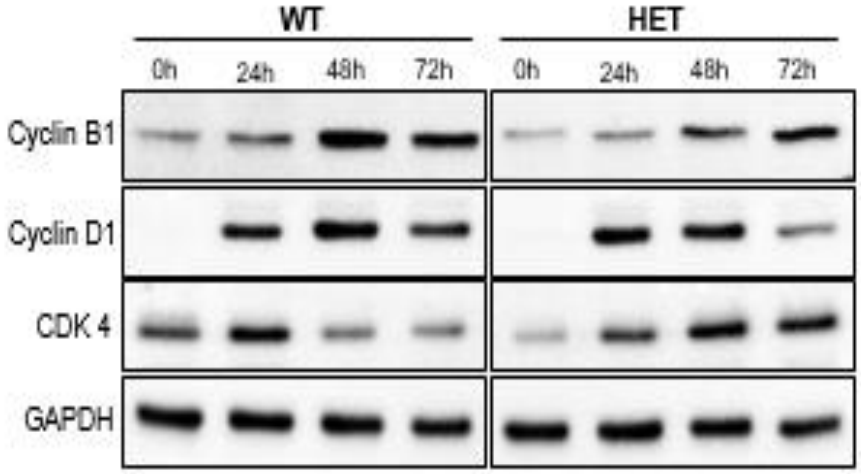
WT
HET
0h
24h
48h
72h
0h
24h
48h
72h
Cyclin B1
Cyclin D1
CDK 4
GAPDH

Figure 2-8. METTL14 depletion downregulates Cell cycle-related protein expression in the liver after PH in mice.

(A) Relative protein expression of Cyclin D1 in the liver after PH in WT and HET mice; n=3, per group. (B) Relative protein expression of CDK4 in the liver after PH in WT and HET mice; n=3, per group. (C) Representative western blot of cyclin B1, cyclin D1 and CDK4 in the liver after PH in WT and HET mice. Values are shown as means ± SD. Significance calculated using unpaired two-tailed student's t-test. *P<0.05, **P<0.01 and ***P<0.001 when compared among time points in same group; #P<0.05, ##P<0.01 and ###P<0.001 when compared between WT and HET mice.

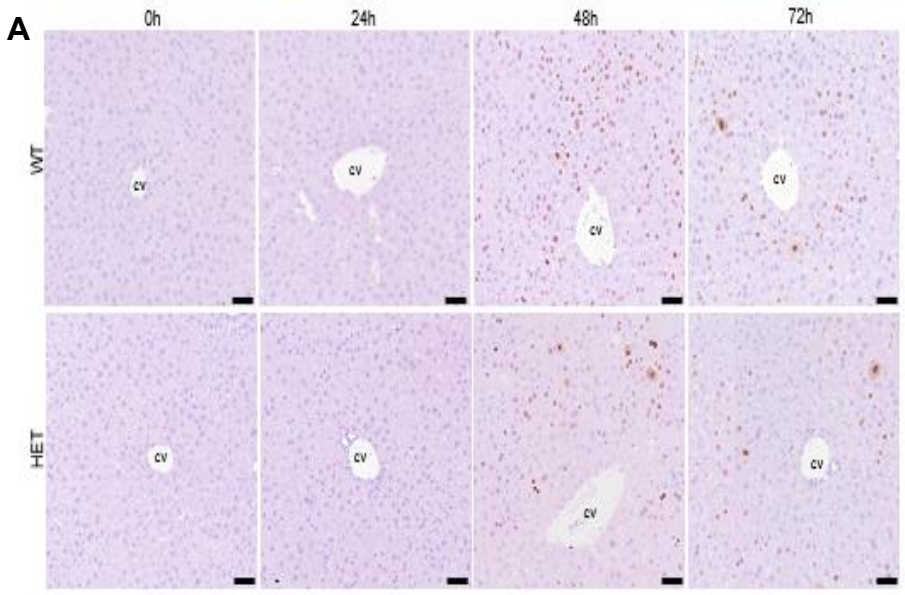
A
0h
24h
48h
72h
WT
HET
cv

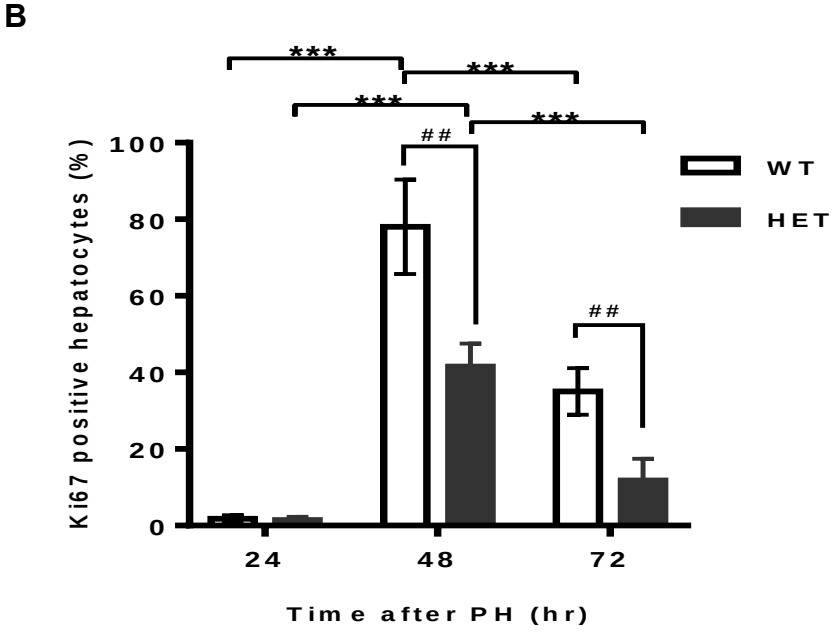
B
***
***
***
***
##
##
100
80
60
40
20
0
Ki67 positive hepatocytes (%)
24
48
72
Time after PH (hr)
WT
HET

Figure 2-9. METTL14 depletion reduces hepatocyte proliferation in liver re-generation after PH.

(A) Representative MKI67-immunohistochemical images and quantifycation of MKI67 staining in hepatocyte nuclei in the liver after PH in WT and HET mice. (B) Quantification of MKI67 staining in hepatocyte nuclei at the indicated time points after PH; n=4, per group. Values are shown as means ± SD. Significance calculated using unpaired two-tailed student's t-test. *P<0.05, **P<0.01 and ***P<0.001 when compared among time points in same group; #P<0.05, ##P<0.01 and ###P<0.001 when compared between WT and HET mice.; Scale bar=50 μm

2.3.3. *Mettl14* mutation induced differentially gene expression regarding liver regeneration after PH.

I investigated the Transcriptomic landscape of regeneration related genes after PH using bulk RNA-seq analysis. Taking conditions of adjusted p-value < 0.05 and absolute value of log2FoldChange > 0.58 as the cutoff for finding DEGs, I investigated time-wise expression pattern of 23 manually selected regeneration related genes and analyzed them by regenerative phase for each genotype mice (Fig 2-10A).

This study revealed that HGF, JAK3, and STAT3, known to stimulate cell cycle progression and hepatocyte proliferation in early phase of liver regeneration, were highly enriched in HET mice after PH[31,32]. During the middle phase of liver regeneration after PH, the expression levels of key cell cycle regulators, including Cyclin B1 (ccnb1), RELB (a subunit of NF-KB), and E2F7, were significantly elevated in HET mice. These findings provide compelling evidence that HET mice exhibit a higher enrichment of critical cell cycle regulatory gene expression during the liver regeneration process.[30]. However, the protein

expression of these genes was decreased and consequently, hepatocyte proliferation was reduced in HET mice compared to WT mice (Fig. 2-8A-C and Fig. 2-9A, B). Furthermore, TGF-β1, which inhibits hepatocyte proliferation and regulate the termination phase of liver regeneration after PH, exhibited high enrichment in HET mice for 72 hours after PH[31]. Another significant finding was that STAT5B, which is known to promote proliferation in breast cancer research, was reduced in WT mice (Fig 2-10A) [63].

Notably, the results demonstrated that hnRNPA2B1, an m^6A binding protein involved in pre-miRNA maturation, mRNA stabilization, mRNA alternative splicing and mRNA translocation, was enriched in WT mice[2]. Conversely, IGF2BP3, another m^6A binding protein associated with mRNA stability enhancement and mRNA translation regulation, was highly enriched in HET mice during liver regeneration after PH[2].

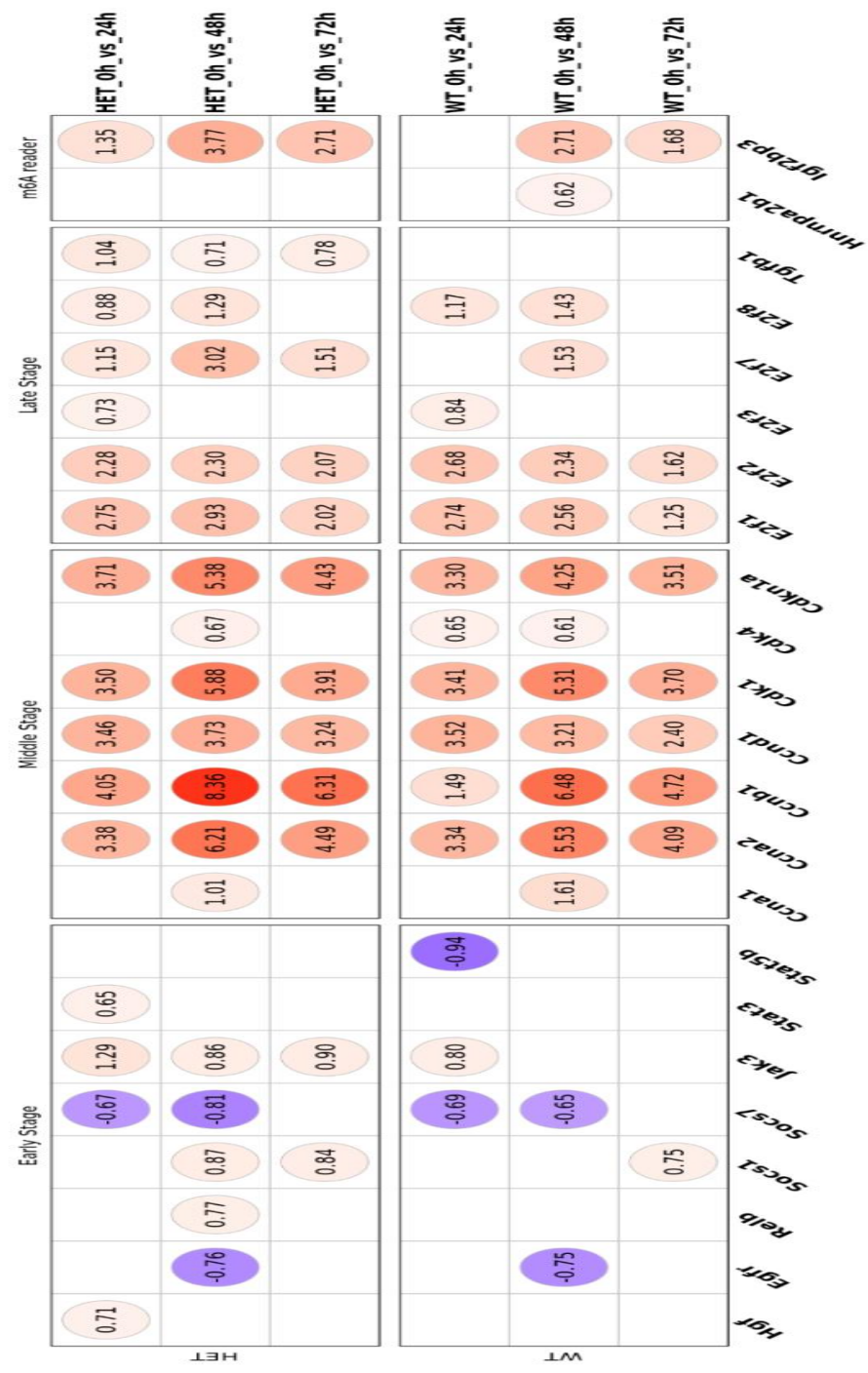
A
HET
WT
Early Stage
Middle Stage
Late Stage
m6A reader
HET_0h_vs_24h
HET_0h_vs_48h
HET_0h_vs_72h
WT_0h_vs_24h
WT_0h_vs_48h
WT_0h_vs_72h
Hnrnpa2b1
Igf2bp3
Tgfb1
E2f8
E2f7
E2f3
E2f2
E2f1
Cdkn1a
Cdk4
Cdk1
Ccnd1
Ccnb1
Ccna2
Ccna1
Stat5b
Stat3
Jak3
Socs7
Socs1
Relb
Egfr
Hgf
0.71
-0.67
1.29
0.65
-0.76
0.77
0.87
-0.81
0.86
0.84
0.90
3.38
4.05
3.46
3.50
6.21
8.36
3.73
5.88
1.01
0.67
4.49
6.31
3.24
3.91
3.71
5.38
4.43
2.75
2.28
0.73
1.15
0.88
1.04
2.93
2.30
0.71
2.02
2.07
1.51
0.78
1.35
3.77
2.71
-0.94
-0.69
0.80
3.34
1.49
3.52
3.41
0.65
3.30
2.74
2.68
0.84
1.17
1.61
5.53
6.48
3.21
5.31
0.61
4.25
2.56
2.34
1.53
1.43
0.62
2.71
-0.75
-0.65
0.75
4.09
4.72
2.40
3.70
3.51
1.25
1.62
1.68

Figure 2-10. Transcriptomic landscape of genes regarding of liver regeneration after partial hepatectomy.

(A) Dot plot of tissue regeneration related genes from transcriptomic analysis of differentially expressed genes (adjusted-p value < 0.05, absolute value of log2FoldChange > 0.58) in liver after partial hepatectomy. log2FoldChange value of each selected DEG is shown in range of colors. Blue color represents down-regulation and red color represents up-regulation compared to 0h group.; n=3 for all group.

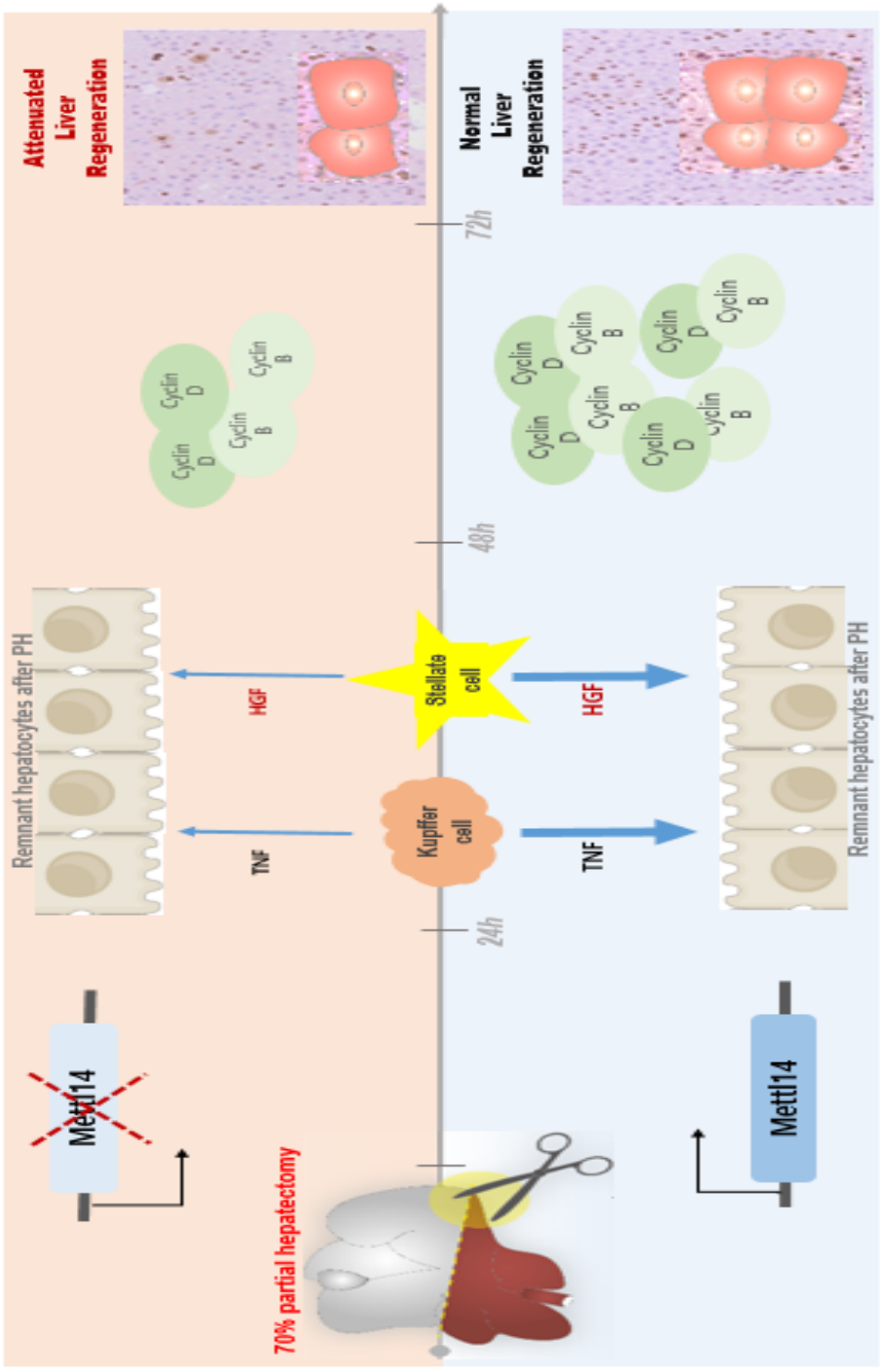
Attenuated Liver Regeneration
Normal Liver Regeneration
72h
48h
24h
Cyclin D
Cyclin B
Remnant hepatocytes after PH
HGF
TNF
Stellate cell
Kupffer cell
Mettl14
70% partial hepatectomy

A

Figure 2-11. *Mettl14* mutation attenuates liver regeneration after PH.

(A) Graphical summary of *Mettl14* expression in liver regeneration after PH.

2.4 Discussion

METTL14 has an important role in endogenous RNA modification as an m^6A methyltransferase[2]. A recent study has shown that METTL14 is involved in liver regeneration following acute injuries, such as PH[16].

The regeneration process after PH is influenced by extensive interaction of parenchymal as well as non-parenchymal cells. The influence of the METTL14-related m^6A modification pathway on non-parenchymal cells, such as sinusoidal endothelial cells, stellate cells, and Kupffer cells, is not yet understood.

In this study, I performed surgical experiments using HET mice, to evaluate the influence of METTL14 on liver regeneration mediated by non-parenchymal liver cells. I found that the liver mass was similar in both the HET and WT mice over 8 weeks of age, as measured by the ratio of their liver weight to body weight (Fig. 2-3A).

My findings are consistent with those of Cao et al.[16], who

showed that liver development in mice with liver-specific Mettl14 knockout was similar that in wild-type mice. However, to confirm whether the liver development in the Mettl14-knockout heterozygous mice we used is normal, more research is required. Meanwhile, the ratio of liver weight to body weight between 24h and 72h after PH was significantly decreased in HET mice compared to WT mice. Furthermore, mRNA expression of HGF, which is a complete mitogen secreted by stellate cells, was down-regulated in HET mice compared to WT mice. In addition, mRNA expression of TNF-α, which is a mitogen released by endothelial cells and Kupffer cells, was significantly decreased in HET mice than in WT mice at 72h after PH.

This experiment focused on the findings at 72h after PH, as most of the active postoperative hepatocellular proliferation occurs during this period[32,61]. Protein expression of these two mitogens was notably reduced at 72h after PH in HET mice compared to WT mice. These results support the hypothesis that METTL14-mediated m^6A modification can affect the expression of certain mitogens derived from non-parenchymal liver cells,

leading to the initiation phase of liver regeneration. In contrast, the protein expression of EGFR was increased at 24h after PH in HET mice compared to WT mice. EGFR is a membrane receptor that binds to EGF, which is one of the complete mitogens secreted from the Brunner' s gland of the duodenum[27,62]. This implies that specific growth factors which involve in extracellular signaling pathway and originate from organs besides the liver are not influenced by the m^6A modification pathway.

Subsequently, I analyzed the cell-cycle pathway, which is stimulated by HGF and TNF-α. The expression of cyclin D1, which is a major regulator of the G1 phase, was downregulated in HET mice compared to the WT mice and was particularly remarkably decreased at 72h after PH. In addition, the expression of cyclin B1, which is a regulator of the mitosis phase, decreased faster in HET mice than in WT mice. These consistent cascading results suggest that the cell cycle is decreased in HET mice. CDK4 is a transcription factor of the G1 phase. My findings revealed that there was a tendency toward upregulation of CDK4 expression in HET mice, unlike that of cell cyclins. This suggests the presence of a compensatory response, which is not affected

by METTL14-mediated m^6A modification. However, further research is needed to validate our findings.

Next, I analyzed the hepatocyte proliferation rate using MKI67-positive hepatocytes, which was significantly decreased in HET mice compared to WT mice, and consistent with the results of the liver weight-to-body weight ratio. In this experiment, I found that novel biological events involving mitogenic pathways, induced by non-parenchymal liver cells, are disturbed by incomplete *Mettl14* expression. Nonetheless, it remains a challenge to prove that HGF and TNF-α are actual targets of *Mettl14* by assessing their RNA transcripts for m^6A enrichment. I believe that additional research into the relationship of non-parenchymal liver cells using conditional *Mettl14* knockout mice will help us overcome the limitations of this work.

Then, I investigated the Transcriptomic landscape of regeneration related genes after PH. In this analysis, I found that TGF-β1 exhibit high enrichment in HET mice throughout liver regeneration after PH. It implicated that Mettl14 inhibits TGF-β signaling during postoperative liver regeneration, Additionally, in

HET mice shows highly enriched IGF2BP3 but hnRNPA2B1. Further experiments are required to validate the findings and gain a better understanding.

Taken together, this study suggested that the m^6A modification is essential in compensatory liver regeneration involving non-parenchymal liver cells after acute injury. Furthermore, these results provide new insights into the existing knowledge on the regenerative processes in the liver following surgical treatment.

Conclusion

This study showed that the ratio of liver weight to body weight between 24h and 72h after PH was significantly decreased in HET mice compared to WT mice. Furthermore, mRNA expression of HGF, which is a complete mitogen secreted by stellate cells, was down-regulated in HET mice compared to WT mice. In addition, mRNA expression of TNF-α, which is a mitogen released by endothelial cells and Kupffer cells, was significantly decreased in HET mice than in WT mice at 72h after PH. This experiment focused on the findings at 72h after PH, as most of the active postoperative hepatocellular proliferation occurs during this period [32,60]. Protein expression of these two mitogens was notably reduced at 72h after PH in HET mice compared to WT mice.

These results support the hypothesis that METTL14-mediated m^6A modification can affect the expression of certain mitogens derived from non-parenchymal liver cells, leading to the initiation phase of liver regeneration (Fig 2-11A).

In this experiment, I found that novel biological events

involving mitogenic pathways, induced by non-parenchymal liver cells, are disturbed by incomplete *Mettl14* expression. Nonetheless, it remains a challenge to prove that HGF and TNF-α are actual targets of *Mettl14* by assessing their RNA transcripts for m^6A enrichment.

References

1. Chen, M., and Wong, C.M. (2020). The emerging roles of N6-methyladenosine (m6A) deregulation in liver carcinogenesis. Mol Cancer *19*, 44. 10.1186/s12943-020-01172-y.

2. Jiang, X., Liu, B., Nie, Z., Duan, L., Xiong, Q., Jin, Z., Yang, C., and Chen, Y. (2021). The role of m6A modification in the biological functions and diseases. Signal Transduct Target Ther *6*, 74. 10.1038/s41392-020-00450-x.

3. Li, J., Zhu, L., Shi, Y., Liu, J., Lin, L., and Chen, X. (2019). m6A demethylase FTO promotes hepatocellular carcinoma tumorigenesis via mediating PKM2 demethylation. Am J Transl Res *11*, 6084-6092.

4. Rong, Z.X., Li, Z., He, J.J., Liu, L.Y., Ren, X.X., Gao, J., Mu, Y., Guan, Y.D., Duan, Y.M., Zhang, X.P., et al. (2019). Downregulation of Fat Mass and Obesity Associated (FTO) Promotes the Progression of Intrahepatic Cholangiocarcinoma. Front Oncol *9*, 369. 10.3389/fonc.2019.00369.

5. Hou, J., Zhang, H., Liu, J., Zhao, Z., Wang, J., Lu, Z., Hu, B., Zhou, J., Zhao, Z., Feng, M., et al. (2019). YTHDF2 reduction fuels infla mma

tion and vascular abnormalization in hepatocellular carcinoma. Mol Cancer *18*, 163. 10.1186/s12943-019-1082-3.

6. Yang, Z., Li, J., Feng, G., Gao, S., Wang, Y., Zhang, S., Liu, Y., Ye, L., Li, Y., and Zhang, X. (2017). MicroRNA-145 Modulates N(6)-Methyladenosine Levels by Targeting the 3'-Untranslated mRNA Region of the N(6)-Methyladenosine Binding YTH Domain Family 2 Protein. J Biol Chem *292*, 3614-3623. 10.1074/jbc.M116.749689.

7. Huang, H., Weng, H., Sun, W., Qin, X., Shi, H., Wu, H., Zhao, B.S., Mesquita, A., Liu, C., Yuan, C.L., et al. (2018). Recognition of RNA N(6)-methyladenosine by IGF2BP proteins enhances mRNA stability and translation. Nat Cell Biol *20*, 285-295. 10.1038/s41556-018-0045-z.

8. Lin, S., and Gregory, R.I. (2014). Methyltransferases modulate RNA stability in embryonic stem cells. Nat Cell Biol 16, 129-131. 10.1038/ncb2914.

9. Shulman, Z., and Stern-Ginossar, N. (2020). The RNA modification N(6)-methyladenosine as a novel regulator of the immune system. Nat Immunol 21, 501-512. 10.1038/s41590-020-0650-4.

10. Hua, W., Zhao, Y., Jin, X., Yu, D., He, J., Xie, D., and Duan, P. (2018).

METTL3 promotes ovarian carcinoma growth and invasion through the regulation of AXL translation and epithelial to mesenchymal transition. Gynecol Oncol 151, 356-365. 10.1016/j.ygyno.2018.09.015.

11. Yang, X., Zhang, S., He, C., Xue, P., Zhang, L., He, Z., Zang, L., Feng, B., Sun, J., and Zheng, M. (2020). METTL14 suppresses proliferation and metastasis of colorectal cancer by down-regulating oncogenic long non-coding RNA XIST. Mol Cancer 19, 46. 10.1186/s12943-020-1146-4.

12. Lin, Z., Hsu, P.J., Xing, X., Fang, J., Lu, Z., Zou, Q., Zhang, K.J., Zhang, X., Zhou, Y., Zhang, T., et al. (2017). Mettl3-/Mettl14-mediated mRNA N(6)-methyladenosine modulates murine spermatogenesis. Cell Res 27, 1216-1230. 10.1038/cr.2017.117.

13. Lu, J., Qian, J., Yin, S., Zhou, L., Zheng, S., and Zhang, W. (2020). Mechanisms of RNA N(6)-Methyladenosine in Hepatocellular Carcinoma: From the Perspectives of Etiology. Front Oncol 10, 1105. 10.3389/fonc.2020.01105.

14. Ma, J.Z., Yang, F., Zhou, C.C., Liu, F., Yuan, J.H., Wang, F., Wang, T.T., Xu, Q.G., Zhou, W.P., and Sun, S.H. (2017). METTL14 suppresses the metastatic potential of hepatocellular carcinoma by modulating N(6) -

methyladenosine-dependent primary MicroRNA processing. Hepatology 65, 529-543. 10.1002/hep.28885.

15. Meng, J., Zhao, Z., Xi, Z., and Xia, Q. (2022). Liver-specific Mettl3 ablation delays liver regeneration in mice. Genes Dis 9, 697-704. 10.1016/j.gendis.2020.11.002.

16. Cao, X., Shu, Y., Chen, Y., Xu, Q., Guo, G., Wu, Z., Shao, M., Zhou, Y., Chen, M., Gong, Y., et al. (2021). Mettl14-Mediated m(6)A Modification Facilitates Liver Regeneration by Maintaining Endoplasmic Reticulum Homeostasis. Cell Mol Gastroenterol Hepatol 12, 633-651. 10.1016/j.jcmgh.2021.04.001.

17. Michalopoulos, G.K., and Bhushan, B. (2021). Liver regeneration: biological and pathological mechanisms and implications. Nat Rev Gastroenterol Hepatol 18, 40-55. 10.1038/s41575-020-0342-4.

18. Kurinna, S., and Barton, M.C. (2011). Cascades of transcription regulation during liver regeneration. Int J Biochem Cell Biol 43, 189-197. 10.1016/j.biocel.2010.03.013.

19. Miyaoka, Y., and Miyajima, A. (2013). To divide or not to divide: revisiting liver regeneration. Cell Div 8, 8. 10.1186/1747-1028-8-8.

20. DeLeve, L.D., Wang, X., and Wang, L. (2016). VEGF-sdf1 recruitment of CXCR7+ bone marrow progenitors of liver sinusoidal endothelial cells promotes rat liver regeneration. Am J Physiol Gastrointest Liver Physiol 310, G739-746. 10.1152/ajpgi.00056.2016.

21. Fujii, H., Hirose, T., Oe, S., Yasuchika, K., Azuma, H., Fujikawa, T., Nagao, M., and Yamaoka, Y. (2002). Contribution of bone marrow cells to liver regeneration after partial hepatectomy in mice. J Hepatol 36, 653-659. 10.1016/s0168-8278(02)00043-0.

22. Bonnardel, J., T'Jonck, W., Gaublomme, D., Browaeys, R., Scott, C.L., Martens, L., Vanneste, B., De Prijck, S., Nedospasov, S.A., Kremer, A., et al. (2019). Stellate Cells, Hepatocytes, and Endothelial Cells Imprint the Kupffer Cell Identity on Monocytes Colonizing the Liver Macrophage Niche. Immunity 51, 638-654.e639. 10.1016/ j.immuni.2019.08.017.

23. Marubashi, S., Dono, K., Asaoka, T., Hama, N., Gotoh, K., Miyamoto, A., Takeda, Y., Nagano, H., Umeshita, K., and Monden, M. (2006). Risk factors for graft dysfunction after adult-to-adult living donor liver transplantation. Transplant Proc 38, 1407-1410. 10.1016/ j.trans proceed.2006.02.091.

24. Mars, W.M., Liu, M.L., Kitson, R.P., Goldfarb, R.H., Gabauer, M.K., and Michalopoulos, G.K. (1995). Immediate early detection of urokinase receptor after partial hepatectomy and its implications for initiation of liver regeneration. Hepatology 21, 1695-1701.

25. Kim, T.H., Mars, W.M., Stolz, D.B., and Michalopoulos, G.K. (2000). Expression and activation of pro-MMP-2 and pro-MMP-9 during rat liver regeneration. Hepatology 31, 75-82. 10.1002/hep.510310114.

26. Nejak-Bowen, K.N., and Monga, S.P. (2013). Wnt drives stem cell-mediated repair response after hepatic injury. Hepatology 58, 1847-1850. 10.1002/hep.26579.

27. Michalopoulos, G.K. (2013). Principles of liver regeneration and growth homeostasis. Compr Physiol 3, 485-513. 10.1002/cphy. c120014.

28. Higgins, G., Anderson, R.E., Higgins, G., and Anderson, R. (1931). Experimental pathology of liver: restoration of liver in white rat following partial surgical removal.

29. Mitchell, C., and Willenbring, H. (2008). A reproducible and well-tolerated method for 2/3 partial hepatectomy in mice. Nat Protoc 3, 1167-1170. 10.1038/nprot.2008.80.

30. Michalopoulos, G.K. (2017). Hepatostat: Liver regeneration and normal liver tissue maintenance. Hepatology 65, 1384-1392. 10.1002/hep.28988.

31. Fausto, N., Campbell, J.S., and Riehle, K.J. (2006). Liver regeneration. Hepatology 43, S45-53. 10.1002/hep.20969.

32. Michalopoulos, G.K. (2007). Liver regeneration. J Cell Physiol 213, 286-300. 10.1002/jcp.21172.

33. Malik, R., Selden, C., and Hodgson, H. (2002). The role of non-parenchymal cells in liver growth. Semin Cell Dev Biol 13, 425-431. 10.1016/s1084952102001301.

34. Akerman, P., Cote, P., Yang, S.Q., McClain, C., Nelson, S., Bagby, G.J., and Diehl, A.M. (1992). Antibodies to tumor necrosis factor-alpha inhibit liver regeneration after partial hepatectomy. Am J Physiol 263, G579-585. 10.1152/ajpgi.1992.263.4.G579.

35. Cressman, D.E., Greenbaum, L.E., DeAngelis, R.A., Ciliberto, G., Furth, E.E., Poli, V., and Taub, R. (1996). Liver failure and defective hepatocyte regeneration in interleukin-6-deficient mice. Science 274, 1379-1383. 10.1126/science.274.5291.1379.

36. Cruise, J.L., and Michalopoulos, G. (1985). Norepinephrine and epidermal growth factor: dynamics of their interaction in the stimulation of hepatocyte DNA synthesis. J Cell Physiol 125, 45-50. 10.1002/jcp.1041250107.

37. Michalopoulos, G.K., and DeFrances, M. (2005). Liver regeneration. Adv Biochem Eng Biotechnol 93, 101-134. 10.1007/b99968.

38. Trusolino, L., Bertotti, A., and Comoglio, P.M. (2010). MET signalling: principles and functions in development, organ regeneration and cancer. Nat Rev Mol Cell Biol 11, 834-848. 10.1038/nrm3012.

39. Gentile, A., Trusolino, L., and Comoglio, P.M. (2008). The Met tyrosine kinase receptor in development and cancer. Cancer Metastasis Rev 27, 85-94. 10.1007/s10555-007-9107-6.

40. Taub, R. (2004). Liver regeneration: from myth to mechanism. Nat Rev Mol Cell Biol 5, 836-847. 10.1038/nrm1489.

41. Yang, I., Son, Y., Shin, J.H., Kim, I.Y., and Seong, J.K. (2022). Ahnak depletion accelerates liver regeneration by modulating the TGF-beta/Smad signaling pathway. BMB Rep 55, 401-406. 10.5483/BMBRep.2022.55.8.071.

42. Baak, J.P. (1990). Mitosis counting in tumors. Hum Pathol 21, 683-685. 10.1016/0046-8177(90)90026-2.

43. Kim, Y.J., Kim, H.J., Lee, W.J., and Seong, J.K. (2020). A comparison of the metabolic effects of treadmill and wheel running exercise in mouse model. Lab Anim Res 36, 3. 10.1186/s42826-019-0035-8.

44. Assy, N., Gong, Y., Zhang, M., Pettigrew, N.M., Pashniak, D., and Minuk, G.Y. (1998). Use of proliferating cell nuclear antigen as a marker of liver regeneration after partial hepatectomy in rats. J Lab Clin Med 131, 251-256. 10.1016/s0022-2143(98)90097-x.

45. Fausto, N., Laird, A.D., and Webber, E.M. (1995). Liver regeneration. 2. Role of growth factors and cytokines in hepatic regeneration. Faseb j 9, 1527-1536. 10.1096/fasebj.9.15.8529831.

46. Bohm, F., Kohler, U.A., Speicher, T., and Werner, S. (2010). Regulation of liver regeneration by growth factors and cytokines. EMBO Mol Med 2, 294-305. 10.1002/emmm.201000085.

47. Natarajan, A., Wagner, B., and Sibilia, M. (2007). The EGF receptor is required for efficient liver regeneration. Proc Natl Acad Sci U S A 104, 17081-17086. 10.1073/pnas.0704126104.

48. Kitamura, T., Watanabe, S., and Sato, N. (1998). Liver regeneration, liver cancers and cyclins. J Gastroenterol Hepatol 13 Suppl, S96-99.

49. Mullany, L.K., White, P., Hanse, E.A., Nelsen, C.J., Goggin, M.M., Mullany, J.E., Anttila, C.K., Greenbaum, L.E., Kaestner, K.H., and Albrecht, J.H. (2008). Distinct proliferative and transcriptional effects of the D-type cyclins in vivo. Cell Cycle 7, 2215-2224. 10.4161/cc.7.14.6274.

50. Fausto, N. (2000). Liver regeneration. J Hepatol 32, 19-31. 10.1016/s0168-8278(00)80412-2.

51. Ledda-Columbano, G.M., Pibiri, M., Concas, D., Cossu, C., Tripodi, M., and Columbano, A. (2002). Loss of cyclin D1 does not inhibit the proliferative response of mouse liver to mitogenic stimuli. Hepatology 36, 1098-1105. 10.1053/jhep.2002.36159.

52. Albrecht, J.H., Hu, M.Y., and Cerra, F.B. (1995). Distinct patterns of cyclin D1 regulation in models of liver regeneration and human liver. Biochem Biophys Res Commun 209, 648-655. 10.1006/bbrc.1995.1548.

53. Boehm, M., and Nabel, E.G. (2001). Cell cycle and cell migration: new pieces to the puzzle. Circulation 103, 2879-2881. 10.1161/01.cir.103.

24.2879.

54. Fu, Y., Dominissini, D., Rechavi, G., and He, C. (2014). Gene expression regulation mediated through reversible m(6)A RNA methylation. Nat Rev Genet 15, 293-306. 10.1038/nrg3724.

55. Jia, G., Fu, Y., and He, C. (2013). Reversible RNA adenosine methylation in biological regulation. Trends Genet 29, 108-115. 10.1016/j.tig.2012.11.003.

56. Michalopoulos, G.K., and DeFrances, M.C. (1997). Liver regeneration. Science 276, 60-66. 10.1126/science.276.5309.60.

57. Bhave, V.S., Paranjpe, S., Bowen, W.C., Donthamsetty, S., Bell, A.W., Khillan, J.S., and Michalopoulos, G.K. (2011). Genes inducing iPS phenotype play a role in hepatocyte survival and proliferation in vitro and liver regeneration in vivo. Hepatology 54, 1360-1370. 10.1002/hep.24507.

58. Mars, W.M., Kim, T.H., Stolz, D.B., Liu, M.L., and Michalopoulos, G.K. (1996). Presence of urokinase in serum-free primary rat hepatocyte cultures and its role in activating hepatocyte growth factor. Cancer Res 56, 2837-2843.

59. Stolz, D.B., Ross, M.A., Salem, H.M., Mars, W.M., Michalopoulos, G.K., and Enomoto, K. (1999). Cationic colloidal silica membrane perturbation as a means of examining changes at the sinusoidal surface during liver regeneration. Am J Pathol 155, 1487-1498. 10.1016/s0002-9440(10)65464-8.

60. Gerlach, C., Sakkab, D.Y., Scholzen, T., Dassler, R., Alison, M.R., and Gerdes, J. (1997). Ki-67 expression during rat liver regeneration after partial hepatectomy. Hepatology 26, 573-578. 10.1002/hep.510260307.

61. Marongiu, F., Marongiu, M., Contini, A., Serra, M., Cadoni, E., Murgia, R., and Laconi, E. (2017). Hyperplasia vs hypertrophy in tissue regeneration after extensive liver resection. World J Gastroenterol 23, 1764-1770. 10.3748/wjg.v23.i10.1764.

62. Olsen, P.S., Poulsen, S.S., and Kirkegaard, P. (1985). Adrenergic effects on secretion of epidermal growth factor from Brunner's glands. Gut 26, 920-927. 10.1136/gut.26.9.920.

63 Liu X, Robinson GW, Hennighausen L. (1996). Activation of Stat5a and Stat5b by tyrosine phosphorylation is tightly linked to mammary gland differentiation. Mol Endocrinol.10(12):1496-1506 /mend.10.12.8961260.

국문 초록

N6-메틸아데노신(m^6A) 변형 경로가 간 재생 및 간세포 암종과 관련이 있다고 보고되었으며, 메틸트랜스퍼라제3(METTL3) 및 메틸트랜스퍼라제14(METTL14)와 같은 m^6A 메틸트랜스퍼라제가 간세포 특이적 재생 경로와 관련이 있다는 것이 밝혀졌 습니다.

간 재생은 복잡한 기전들이 관여하여 신체의 항상성을 유지할 수 있도록 적정한 비 율을 유지하며 재생하고, 특정 조건이 되면 재생을 멈추는 놀랄 만큼 체계적인 생리학적 현상입니다. 이런 고유한 특징에 대해 지금까지 많은 연구가 수행되었음에도 불구하고 간재생에 대한 전 과정을 완전히 이해한 것은 아닙니다.

본 연구에서는 간 재생의 복잡한 과정에서 간세포와 관련된 METTL14의 역할을 설명하기 위해 Mettl14 녹아웃(Knock-out) 형질전환 마우스의 이형접합체(Hetero-zygous) 마우스 및 야생형(Wild-type) 마우스에서 70%의 간을 절제하는 부분 간절 제술(Partial hepatectomy)을 수행했습니다. 다음으로, 체중에 대한 간 중량의 비율과 비실질 간 세포에서 유래한 유사분열 촉진제의 발현을 분석하였습니다. 또한 MKI67 면역염색을 통해 세포주기 관련 유전자의 발현과 간세포 증식률을 평가했습니다. 부분 간절제술 후 재생하는 과정에서 체중 대비 간 무게의 비율은 야생형 마우스에 비해 Mettl14

형질전환 마우스에서 더 낮았습니다. 비실질 간세포에서 유래하며 세포주기를 자극하는 미토겐 (mitogen)인 간세포성장 인자(HGF)와 종양괴사 인자(TNF)-알파, 세포주기를 조절하는 사이클린 B1, D1의 발현 및 후기 G1-M 단계의 증 식성 간세포를 나타내는 MKI67-양성 세포의 수는 Mettl14 변이 마우스에서 부분 간 절제술 이후 72시간째에 유의하게 감소하였습니다.

본 연구로 Mettl14 유전자의 감소가 굴모세혈관 내피세포 (sinusoidal endothelial cell), 간별세포(hepatic stellate cell) 및 별큰포식세포(Kupffer cell)에서 파생된 H GF 및 TNF-α와 같은 특정 미토겐의 발현을 억제함으로써 부분 간절제술과 같은 급성 손상을 받은 간의 재생과정을 저해할 수 있다는 것을 확인하였습니다.

이러한 결과는 Mettl14의 간 재생에 관여하는 역할에 대한 새로운 통찰력을 제시하고 더 나아가 간 재생과 관련된 질환의 새로운 치료 지표로서의 가능성을 제공합니다.

.....

주요어: N6-메틸아데노신, 메틸트랜스-퍼라제 14, 메틸트랜스퍼라제 14 이형 접합체 형질전환 마우스, 간절제술, 간별세포, 별큰포식세포, 간세포성장인자, 종양괴사인자-알파

학 번: 2017-19705

Acknowledgement

“사람이 마음으로 자기의 길을 계획할지라도 그의 걸음을 인도하시는 이는 여호와시니라”(잠언 16, 9).

먼저, 이 모든 것을 계획하시고 인도해 주신 하나님께 찬양과 감사를 올립니다.

긴 여정이었습니다. 2007 년에 학위과정을 시작한 저는 2023 년 8 월에 그 여정을 마무리하게 되어 매우 감격스럽고 감사한 마음이 듭니다.

긍정적인 마음가짐과 끈기를 유산으로 물려주신 양만교님과 故홍후남님 덕분에 박사졸업의 결실을 맺게 되었습니다. 중년의 막내딸을 위해 여전히 마른자리를 살펴 주시는 아빠와 사무치게 그리운 엄마께 무한한 존경과 감사와 사랑을 전합니다.

나의 영원한 동반자이며 멘토이신 최종영 선배님과 훌쩍 자라 예비수의사가 된 최용준군, 우주를 품고 사는 우리의 기대주 최혜준양에게 큰 감사와 사랑을 전합니다. 언제나 저를 지지해 주시는 양문숙님, 양은숙님, 양주민님, 윤미라님과 사랑하는 조카들에게도 깊은 감사의 마음을 전합니다. 또한, 시부모님과 최종우님, 권옥희님, 최현정님, 최원준, 최익준과 이 기쁨을 함께 하고 싶습니다.

이 학위과정에 많은 도움을 주신 신재훈님, 김연주님, 김경은님, 김경훈님, 이상규님, 김상아님, 남미현님, 이정민님을 비롯한 발생유전학교실 식구들께 진심으로 감사드립니다.

졸업하기까지 진심 어린 가르침을 주신 이순신 교수님, 남기택 교수님, 강병철 교수님, 오승현 교수님, 김현석 교수님, 윤준원 교수님, 김미영님, 김종란님, 황지연님, 주영신님, 송은주님께도 진심으로 감사드립니다.

그리고, 논문심사를 위해 아낌없는 격려와 조언을 주신 윤여성 교수님, 류덕영 교수님, 이미옥 교수님, 구승회 교수님께도 깊은 감사를 드리고 싶습니다.

끝으로, 멋진 리더로서 귀감과 영감을 주시고 학업적 성과를 이루게 해 주신 성제경 지도교수님께 감사와 영광을 돌립니다. 감사합니다.